Selectivity in the Photo-Fries Rearrangement of Some Aryl Benzoates in Green and Sustainable Media. Preparative and Mechanistic Studies

Gastón Siano,[†] Stefano Crespi,[‡] Mariella Mella,[‡] and Sergio M. Bonesi*,[†,‡]

[†]Departamento de Química Orgánica, CIHIDECAR − CONICET, Facultad de Ciencias Exactas y Naturales, University of Buenos Aires, 3er Piso, Pabellón 2, Ciudad Universitaria, Buenos Aires 1428, Argentina

[‡]Dipartimento di Chimica, University of Pavia, Sezione Chimica Organica, v.le Taramelli 12, 27100 Pavia, Italy

S *Supporting Information*

ABSTRACT: Irradiation of a series of *p*-substituted aryl benzoates under N_2 atmosphere in homogeneous and micellar media was investigated by means of steady-state condition and of time-resolved spectroscopy. A notable selectivity in favor of the 2-hydroxybenzophenone derivatives was observed in micellar media. The benzophenone derivatives were the main photoproduct. On the other hand, in homogeneous media (cyclohexane, acetonitrile, and methanol) the observed product distribution was entirely different, viz. substituted 2-hydroxybenzophenones, *p*-substituted phenols, benzyl and benzoic acid were found. The binding constants in the surfactant were also measured and NOESY experiments showed that the aryl benzoates were located in the hydrophobic core of the micelle. Laser flash photolysis experiments led to the characterization of both *p*-substituted phenoxy radical and substituted 2-benzoylcyclohexadienone transients in homogeneous and micellar environment.
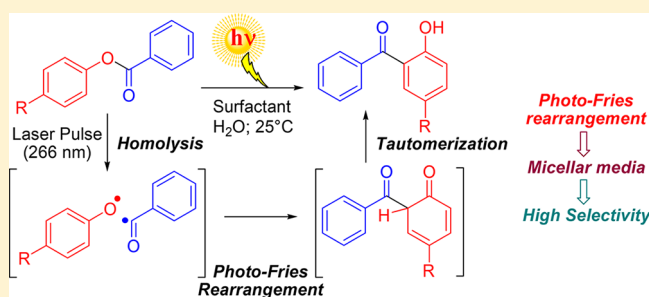
■ INTRODUCTION

Photochemical reactions grant access to a variety of scaffolds difficult, if not impossible, to access through thermal chemistry. However, the energetic advantage of populating the excited states is often paid with a lack of selectivity in product formation. For this reason, reactions involving intermediates such as radical pairs or radical-ion pairs represent a significant challenge regarding product distribution for the synthetic organic photochemist. Zeolites, micelles, polyolefin films, cavitands, dendrimers, etc., as a useful heterogeneous media, can be helpful to direct the selectivity of photoproducts in photoinduced reactions.[1]

Surfactants are amphiphilic molecules and aggregation in solution to form micelles can be achieved when their concentration is 100 times higher than the critical micellar concentration (*cmc*). Then, micelles solubilize efficiently hydrophobic compounds in water, albeit micelles are not static species showing a dynamic equilibrium.[2] Also, micelle can concentrate guest molecules into relatively small effective volumes promoting their re-encounter consequently.[1c] Inside the homophobic core of the micelles, significant cage effects are observed when compared to homogeneous media, with magnitudes impossible to explain considering the sole micro-viscosity in the constrained environment. The main reason for this behavior is based on the hydrophobicity of the solutes where inhibition of their diffusion into the aqueous phase is noteworthy. Thus, the reaction intermediates show a high lifetime in the restricted hydrophobic core of the micelle. For example, geminate radical pairs that are produced photochemically within the micellar core, have their rotational and translational mobility constrained inside the micelles.[2] Indeed, the mobility restricted within the hydrophobic cores of radicals, radical cations, or other reactive intermediates limits unwanted reactions (e.g., radical−radical self-quenching reactions) and the access of adventitious reagents (e.g., water and oxygen) that would cause their collapse in solution. Therefore, micellar solution can induce a product distribution and a relative chemical yield that can be significantly different when compared with homogeneous conditions.[1,2]

There have been many studies on the control of the reactivity of radical species generated within the hydrophobic core of the micelle, and some physical parameters (e.g., electrostatic, polarity, hydrophobic interactions, viscosity, as well as hydrogen-bonding solvation) may be involved in determining their reactivities.[3] In addition, several studies directed to analyze and quantify the reactivity, selectivity, and efficiency of micellar cage on photochemical reactions in water have been carried out.

Among the vast number of photochemical transformations, a particular example is represented by the photo-Fries rearrangement. Anderson and Reese[4] have discovered the photoreaction where a homolytic fragmentation of a carbon−heteroatom bond

A

is involved, i.e., C−O, C−S, and C−N, of esters, thioesters and amides, respectively.[5] The photo-Fries rearrangement proceeds via a well-established radical mechanism, mainly occurring through the excited singlet state.[1b,6] Typically, the photoinduced Fries rearrangement reaction of (hetero)aryl benzoates in homogeneous media affords *ortho-* and *para*-regioisomers as well as the corresponding phenols (Scheme 1).[7,1b]
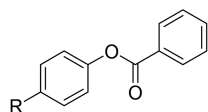
Scheme 1. Photochemisytry of aryl benzoates
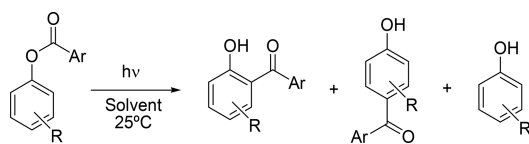
The product distribution of the photo-Fries rearrangement underlines the competition between in-cage radical recombination versus out-of-cage diffusion, and consequently, aryl esters, as model substrates, have been chosen to study heterogeneous environments.[8] In these studies, SDS (sodium dodecyl sulfate) was the preferred surfactant to be tested. In the literature, there are examples of photo-Fries reactions, i.e., irradiation of benzamides in SDS solution and irradiation of aqueous solutions of acetanilides confined in cyclodextrin.[8b,d] Recently, we have studied the photo-Fries rearrangement of a variety of substituted acetanilides in micellar solution showing the high selectivity of the photoreaction in favor of the *ortho*-rearranged photoproducts, viz. substituted 2-aminoacetophenones.[9] The preparation of benzoyloxy benzophenone derivatives requires the use of 2-hydroxybenzophenones as key compounds, demonstrating biological activity and pharmaceutical properties (e.g., antiinflammatory and estrogenic activity).[10] Therefore, we carried out the systematic study the photo-Fries rearrangement of a series of *para*-substituted phenyl benzoates in surfactant solutions with the aim of evaluating the selectivity toward formation of 5-substituted 2-hydroxybenzophenones in a constrained environment. Scheme 2 shows the structures of the surfactants as well as the aryl benzoates employed in this systematic study.

In the present paper, we describe the results on the photo-Fries rearrangement of several *para*-substituted aryl benzoates in homogeneous and micro-heterogeneous media. The binding constants (K_b) and the location of the substrates within micelles are measured through spectroscopic methods. From a preparative point of view, the use of anionic and neutral surfactant micelles shows a high selectivity in favor of the formation of the 2-hydroxybenzophenone derivatives achieving yields higher than 90%. From a mechanistic viewpoint, it furnishes the characterization of both *para*-substituted phenoxy radical and substituted 2-benzoylcyclohexadienone transients in homogeneous and micellar environments. The in-cage and out-of-cage rate constants (k_R and k_E, respectively) of *para*-substituted phenoxy radicals are measured for the first time by means of laser flash photolysis.
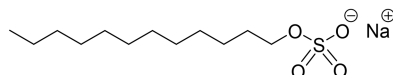
■ RESULTS

Steady-State Photolysis. *Photoirradiation of Aryl Benzoates in Homogeneous Media.* Irradiation of aryl benzoates (**1−8**) in cyclohexane, MeOH, and MeCN, which were chosen as representative nonpolar, protic polar, and aprotic polar solvents, with λ_{exc} = 254 nm under N_2 atmosphere provided the expected photoproducts from the photo-Fries rearrangement, viz. formation of 2-hydroxybenzophenone derivatives (**1a−8a**), the corresponding phenols (**1b−8b**), and benzoic acid. The photochemical reaction is depicted in Scheme 3. The formation

Scheme 3. Photoinduced Fries rearrangement of aryl benzoates (1 − 8)
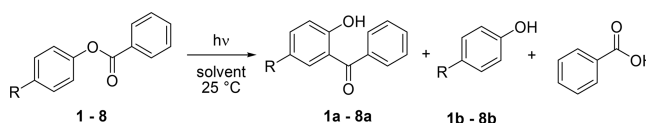
of benzoic acid was attributed to the oxidation of benzaldehyde, which is the primary photoproduct formed, because of the presence of residual molecular oxygen in the reaction mixture.[11] In all of the performed reactions, the yield of benzoic acid was between 5 and 15%.

When esters are consumed, the chemical yields collected in Table 1 show that benzophenones **1a−8a** are the main photoproducts in up to 94% yield. Furthermore, the product distribution did not change significantly with the nature of the solvent, and poor selectivity in favor of the benzophenone derivatives was observed.

The quantum yields of consumption of the aryl benzoates (ϕ_r) in polar and nonpolar solvents were measured (see Table 1). The ϕ_r values were found to be higher than 0.30, implying that the photo-Fries rearrangement reaction occurred efficiently. Moreover, in every solvent, a marked increase of the ϕ_r values was observed, moving from esters bearing electron-donor to

Scheme 2. Structures of surfactants and aryl benzoates

(a) Structures of aryl benzoates.

1 R = OCH$_3$; **2** R = OPh; **3** R = CH$_3$; **4**; R = *t*-Bu;
5 R = H; **6** R = Ph; **7** R = CN; **8** R = NO$_2$
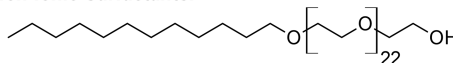
(b) Structures of surfactants.

Anionic Surfactant.

Sodium dodecyl sulfate (SDS)
*cmc*: 8.2 mM

Non-ionic Surfactants.

Polyoxyethylene(22)lauryl ether (Brij P35)
cmc: 0.09 mM

Table 1. Irradiation of Aryl Benzoates in Homogeneous Solution: Yield of Photoproducts,[a] Reaction Quantum Yield (ϕ_r),[b] and Fluorescence Quantum Yield (ϕ_f)[c]

| aryl benzoates | solvent | photoproduct yield (%) | | ϕ_r | ϕ_f |
		benzophenones (a)	phenols (b)		
1	cyclohexane	46	27	0.30	0.08
	MeCN	62	17	0.36	0.03
	MeOH	66	17	0.33	0.10
2	cyclohexane	55	28	0.37	0.002
	MeCN	69	19	0.71	0.013
	MeOH	73	23	0.44	0.002
3	cyclohexane	42	22	0.40	0.25
	MeCN	94	5	0.62	0.07
	MeOH	80	20	0.31	0.11
4	cyclohexane	59	27	0.50	0.001
	MeCN	95	5	0.35	0.025
	MeOH	75	25	0.63	0.002
5	cyclohexane	40[e]	30	0.36	0.001
	MeCN	60[e]	33	0.14	0.005
	MeOH	58[e]	26	0.14	0.002
6	cyclohexane	41	23	0.59	0.012
	MeCN	73	18	0.32	0.035
	MeOH	85	14	0.31	0.033
7	cyclohexane	38	19	0.51	0.002
	MeCN	84	15	0.82	0.025
	MeOH	75	26	0.93	0.002
8	cyclohexane	31	34	0.02	NF[d]
	MeCN	60	40	0.07	NF
	MeOH	50	52	0.07	NF

[a]Yield of photoproducts determined by ^{1}H NMR spectroscopy in the reaction mixture. Concentration of aryl benzoates: 5.0×10^{-3} M. [b]Actinometer: KI (0.6 M), KIO$_3$ (0.1 M) and Na$_2$B$_4$O$_7$.10H$_2$O (0.01 M) solution in water; ϕ (I$_3^-$) = 0.74; λ_{exc} = 254 nm.[12] Error: ±0.01. [c]Actinometer: 4-chloroanisole acetonitrile solution under Ar atmosphere; ϕ_f = 0.019.[13] Error: ±0.002. [d]NF: nonfluorescent substrate. [e]4-Hydroxybenzophenone is also formed: Cyclohexane 30%; MeCN 7%; MeOH 15%.

esters substituted with electron-acceptor substituents. The only exception found was ester **8**. The ϕ_r values measured for compound **8** are lower than 0.10 in all the solvents studied. The aryl benzoates are all poorly fluorescent chromophores (see Table 1) with the exception of benzoate **8** that was found to be nonfluorescent. The spin coupling effect of the nitro group explains the peculiarity of ester **8**.[14,15] Indeed, intersystem crossing pathway competes with both the photo-Fries rearrangement reaction and the fluorescence emission.

UV−vis and NMR spectroscopies were used to follow the photochemical reaction, and aryl benzoates **1**, **2**, **3**, and **7** have been chosen as representative examples for such spectroscopic studies. Figure 1a showed the time-resolved UV−vis absorption spectrum of the photoreaction of *p*-methylphenyl benzoate (**3**) in cyclohexane showing the growth of a new band located at 352 nm during the irradiation time. This band was assigned to the *n*,π* transition of the carbonyl group of benzophenone **3a**[14] and was also observed in MeOH and MeCN. However, no significant solvent effect was observed in the maximum wavelength of the *n*,π* transition band upon change of the solvent polarity. A similar solvent effect on the maximum wavelength of the *n*,π* band of the 2-hydroxybenzophenone derivatives (**1a**, **2a**, **4a−8a**) was also observed (see Figure S1, Supporting Information). On the other hand, a noticeable

substituent effect on the *n*,π* band of the substituted 2-hydroxybenzophenones (**1a−8a**) was observed. In fact, a hypsochromic effect ($\Delta\lambda$ = −73 nm) ascribed to the *n*,π* band was measured by changing the substituent from the electron donor MeO (λ_{max} = 378 nm) to the electron acceptor NO$_2$ (λ_{max} = 305 nm). The course of the photoreaction of ester **1** is detailed in Figure 1b, where the benzoyl [1,3]-migration to form benzophenone **1a** is shown to be the primary process. Parts c and d of Figure 1 show the relative formation of benzophenones **2a** and **7a** (starting from the corresponding esters **2** and **7**), respectively, in nonpolar and polar solvents. The relative rates of formation of **2a** are similar in MeCN and cyclohexane, while in MeOH the rate somewhat lower, implying that in protic polar solvent radiative and nonradiative decay rates compete with the photoreaction pathway. The rates of formation of benzophenone **7a** are quite similar in all of the solvents tested. For the other esters studied, the relative rates of formation of the corresponding benzophenone derivatives showed a similar behavior (see Figure S2, Supporting Information).

The ^{1}H NMR spectra of the photoreaction mixture (6 h irradiation) of 4-cyanophenyl benzoate (**7**) in cyclohexane under N$_2$ atmosphere were also recorded (see Figure S3, Supporting Information). As expected, the formation of the photoproducts benzophenone **7a** and phenol **7b** was confirmed through their diagnostic signals (see Figure S3, Supporting Information) along with the unreacted ester **7**. The experiments demonstrated poor selectivity of the photoreaction in homogeneous media, and this trend was observed for all the esters (**1−8**) studied (see Table 1).

Photoirradiation of Aryl Benzoates in Micellar Media. Irradiation of aryl benzoates (**1−8**) in aqueous SDS (0.10 M) with λ_{exc} = 254 nm under air caused the selective generation of 2-hydroxybenzophenone derivatives (**1a−8a**) in high yields along with lower amounts of the corresponding phenols (**1b−8b**) (for structures, refer to Scheme 3). In these experiments, consumption up to 95% of aryl benzoates (**1−8**) was obtained. The chemical yields of benzophenone derivatives (**1a−8a**) are collected in Table 2.

As is apparent from Table 2, SDS and Brij-P35 micellar solutions promoted a high selectivity on the photo-Fries rearrangement of the aryl benzoates **2−8**, favoring the formation of the corresponding substituted benzophenones (**2a−8a**) over the *para*-substituted phenols. The observed selectivity was attributed to the confinement of the aryl benzoates and the radicals formed after the C−O bond cleavage within the hydrophobic core provided by the micellar medium. Moreover, the *para*-substituted phenols were formed in a minor extent or not formed at all, evidencing the suppression of products arising from cage escape. It is worth noticing that the irradiation of *p*-nitrophenyl benzoate (**8**) gave 2-hydroxy-5-nitrobenzophenone (**8a**) only in 44% yield (the consumption of the starting material was 66% after 6 h of irradiation). No *p*-nitrophenol was detected in the reaction mixture. Competitive deactivation of the singlet state of *p*-nitrophenyl benzoate (**8**) through intersystem crossing accounted for the observed chemical yield of benzophenone **8a**.[14] The competitive process populates the triplet excited state, due to the spin−orbit coupling provided by the nitro group, which is an unproductive excited state of benzoate **8**.

Quantum yields of consumption of the aryl benzoates (ϕ_r, see Table 2) were measured in micellar media, viz. SDS and Brij-P35, and were found to be of the same order of magnitude.
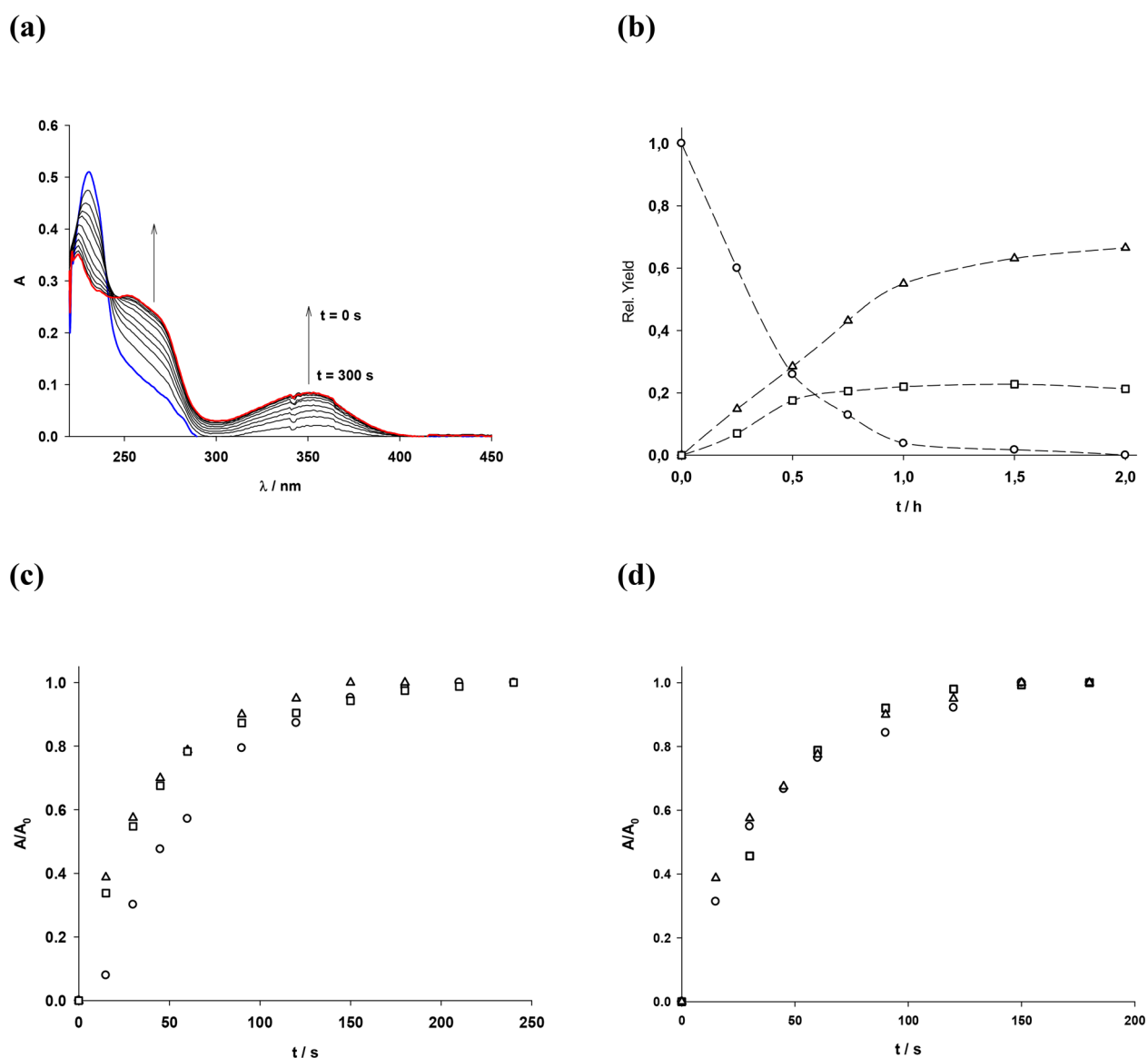
(a)

(b)

(c)

(d)

Figure 1. (a) Time-resolved UV−visible absorption spectrum of **3** in cyclohexane. Blue line: initial time; red line: 300 s. (b) Relative yield profile vs time of **1** in MeOH: ester **1** (circles); benzophenone **1a** (triangles); phenol **1b** (square). (c) Relative absorbance at 358 nm (A/A_∞) of formation of **2a** in MeOH (circles); MeCN (triangles); cyclohexane (square). (d) Relative absorbance at 333 nm (A/A_∞) of formation of **7a** in MeOH (circles); MeCN (triangles); cyclohexane (square).

234 However, the quantum yields measured in SDS solution were
235 larger than in Brij-P35 solutions. This behavior can be attributed
236 to an enhancement of the nonradiative pathway from the singlet
237 state of the aryl benzoates in Brij-P35 solutions. The high-
238 consumption quantum yields and low or no fluorescence
239 emission from aryl benzoates (**1**−**8**) was consistent with a fast
240 reaction from the singlet state. However, nonradiative and
241 intersystem crossing pathways from the singlet state compete
242 with the photo-Fries rearrangement.
243 UV−vis spectroscopy was used for following the photo-
244 reaction and *p*-methoxyphenyl benzoate (**1**) was selected as a
245 representative aryl benzoate. Thus, the reaction of **1** in SDS
246 (0.10 M) was followed by UV−vis absorption spectroscopy, and
247 the UV−vis spectral change vs time is shown in Figure 2a. It is
248 apparent from the UV−vis spectra that the photo-Fries
249 rearrangement of compound **1** to form 2-hydroxy-5-methox-
250 ybenzophenone (**1a**) is the primary process, according to the
251 appearance of the characteristic *n,π** band of the carbonyl group

located at 372 nm. Similar behavior was observed for 252
compounds **2**−**8** (see Figure S1, Supporting Information). 253
The course of the photoreaction of ester **1** is depicted in 254
Figure 2b and clearly shows that the benzoyl [1;3]-migration to 255
form benzophenone **1a** is the main process. On the other hand, 256
we selected aryl benzoates **7** and **4** as examples of aryl benzoates 257
to show the relative formation of benzophenones **7a** and **4a**, 258
respectively, in cyclohexane and 0.10 M SDS and 0.01 M Brij- 259
P35 solutions (see Figure 2c,d). The relative rates of formation 260
of **7a** in surfactant media (see Figure 2c) are slightly lower than 261
in cyclohexane and can be attributed to the radiative and 262
nonradiative decay rates that compete with the photoreaction 263
pathway. Similar behavior is observed for the rates of formation 264
of benzophenone **4a** (see Figure 2d) as well as with for the other 265
benzophenone derivatives (see Figure S2, Supporting Informa- 266
tion). 267
The photoreaction of compound **1** in micellar environment 268
(SDS 0.10 M) was also followed by NMR spectroscopy. The ¹H 269

Table 2. Irradiation of Aryl Benzoates in Micellar Solution: Yield of 5-Substituted 2-Hydroxybenzophenones,[a] Reaction Quantum Yield (ϕ_r),[b] and Fluorescence Quantum Yield (ϕ_f)[c] of Aryl Benzoates

| benzophenones | photoproduct yield (%) | | ϕ_r | | ϕ_f |
	SDS	Brij-P35	SDS	Brij-P35	SDS
1a	94	95	0.13	0.12	0.026
2a	76	85	0.79	0.21	0.026
3a	70	92	0.55	0.41	0.024
4a	85	89	0.54	0.26	0.025
5a	90[e]	92[e]	0.50	0.21	0.029
6a	87	90	0.53	0.21	0.062
7a	80	78	0.45	0.10	0.024
8a	44	56	0.13	0.01	NF[d]

[a]Yield of photoproducts determined by ^{1}H NMR spectroscopy in the reaction mixture. Concentration of aryl benzoates: 5.0×10^{-3} M. [b]Actinometer: KI (0.6 M), KIO$_3$ (0.1 M) and Na$_2$B$_4$O$_7$·10H$_2$O (0.01 M) solution in water; $\phi(I_3^-) = 0.74$; $\lambda_{exc} = 254$ nm.[12] Error: ± 0.01. [c]Actinometer: 4-chloroanisole acetonitrile solution under Ar atmosphere; $\phi_f = 0.019$;[13] Error: ± 0.002. [d]NF: nonfluorescent substrate. [e]4-Hydroxybenzophenone is also formed in 8−10%.

NMR spectra of the reaction mixture of benzoate **1** in SDS (0.10 M) irradiated during 6 h with λ_{exc}= 254 nm (see Figure S4, Supporting Information) showed that benzophenone **1a** was formed in 94% yield along with *p*-methoxyphenol and benzoic acid in yields lower than 5%. In the same spectra, the signals belonging to the surfactant (SDS) were also observed. The consumption of benzoate **1** was quantitative. Similar results were obtained with all the aryl benzoates studied (**2−8**), and the photoproduct yields are collected in Table 2.

Binding Constants (K_b) of Aryl Benzoates in Micellar Media. When ionic and neutral surfactant solutions are used as microreactors to perform photoreactions the knowledge of the reactant's location in the micellar system is required. In order to know the reactant's positioning within micelles, UV−vis and ^{1}H NMR studies of guest molecules (aryl benzoates) in micellar solution were conducted. UV−vis spectroscopy was used to determine the binding constant (K_b) between micelles and aryl benzoates, applying a methodology that has been reported previously for aryl acetamide.[9] Both bathochromic and hyperchromic shifts of the lower energy absorption banrd of the aryl benzoates were observed by addition of increasing amounts of surfactant, demonstrating the binding of the substrates to the micelle that took place within the hydrophobic core of the micelle. Indeed, the binding of the aryl benzoates to the micelle can be described as equilibrium, and K_b can be written according to eq 1, where S represents the benzoates, Surf the surfactants, and [S−Surf] the complex formed between benzoates and the surfactants.

$$[S] + [Surf] \underset{}{\overset{K_b}{\rightleftharpoons}} [S\text{−}Surf] \quad k_b = \frac{[S\text{−}Surf]}{[S][Surf]} \tag{1}$$
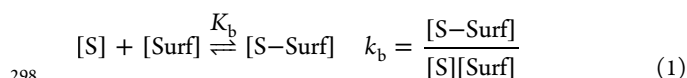
Equation 2 was obtained after application of the Lambert−Beer law on eq 1. A_0 and A are the absorbances at the maximum wavelength in the absence and presence of surfactant, respectively. The molar absorptivity of the complex and the benzoates are dubbed accordingly ε_C and ε_S. A linear relationship is observed between $(A - A_0)^{-1}$ and the reciprocal of the concentration of the surfactant in eq 3, which was obtained after rearranging eq 2.

$$\frac{(A - A_0)}{A_0} = \frac{\varepsilon_C K_b[Surf]}{\varepsilon_S(1 + K_b[Surf])} \tag{2}$$

$$\frac{A_0}{(A - A_0)} = \frac{\varepsilon_S}{\varepsilon_C} + \frac{\varepsilon_S}{\varepsilon_C K_b}\frac{1}{[Surf]} = A_0\frac{1}{\Delta A} \tag{3}$$

The experimental data obtained for some aryl benzoates and SDS and Brij-P35 are shown in Figure 3, and the best linear regression curves are also included in the same figure. The plots for the other systems are collected in Figure S5 (see the Supporting Information). The K_b values for **1−8** calculated from the ratio between the slope and the intercept of the regression curve are shown in Table 3. From these data, it is apparent that the benzoates bind to the micelles, and the ones possessing hydrophobic character, i.e., benzoates **1** and **4** in SDS micellar solution, show high K_b values. Likewise, benzoates **1**, **4**, and **7** possess greater K_b compared to the other substrates in the case of Brij-P35 micellar solution. Generally, the K_b values obtained for benzoates **1−8** are typical of aromatic solutes as it pointed out by Quina, Treiner, and co-workers.[16] Estimation of K_b values ≤100 M^{-1} in SDS for weakly hydrophobic substrates such as phenyl chloroformate have also been reported.[17] Likewise, K_b values have been reported for the binding of Brij-P35 surfactant and a series of benzoyl chloride derivatives, and they were found to be higher than those obtained for other surfactants such as SDS and CTAC.[18] Estimation of a minimum value around 190 M^{-1} for the binding constant (K_b) of Brij-P35 surfactant was reported and accounts for a more apolar environment when pyrene was used as a micropolarity probe.[18]

2D NMR spectroscopy has been recorded to confirm qualitatively the location of the aryl benzoates within the micelle. NOESY experiments have been often used to determine the localization of substrates inside the micelle as well as to determine the extent of coaggregation between two different kinds of surfactants in water.[19] Positive results are achieved when cross-peaks between diagnostic signals of the substrate and the surfactants, respectively, are observed in the corresponding contour plots.[9] Thus, the NOESY experiments were performed in D$_2$O, and Figure 4 shows the 2D NMR spectrum for a solution of SDS (7 mM) in the presence of benzoate **1** (10 mM). The inset red frames recognize the NOE (nuclear Overhauser effect) between the signals of the surfactant SDS (bulk hydrogens and α hydrogen) and the signals belonging to the aromatic protons (H-2/H-6, H-3/H-5, H-10/H-14, H-12, and H-12/H-13) of *p*-cyanophenyl benzoate **7**. Also, Figure 6 shows the labels of the protons of the surfactant SDS and the aryl benzoate **7**, respectively. Similar spectroscopic behavior was observed for solutions of SDS and Brij-P35 in D$_2$O in the presence of aryl benzoates **1** and **3** (see Figures S6−S8, Supporting Information). The cross-peaks of diagnostic signals observed in the 2D NMR contour plots are in agreement with and reinforce the UV−vis spectroscopic analyses.

However, we cannot estimate the location of the benzoates with accuracy but we can suggest that the benzoates are located inside the hydrophobic core of the micelle because the proton nuclei of the aryl benzoates correlate nicely with the proton nuclei of the surfactants as can be seen through the cross-peaks of the contour plots.

Laser Flash Photolysis of Aryl Benzoates. Irradiation of *p*-methoxyphenyl benzoate (**1**) in acetonitrile and cyclohexane solutions with a laser pulse (266 nm) under nitrogen atmosphere gives the transient absorption spectra shown in Figure 5a,b. Four absorption bands with maximum wavelengths
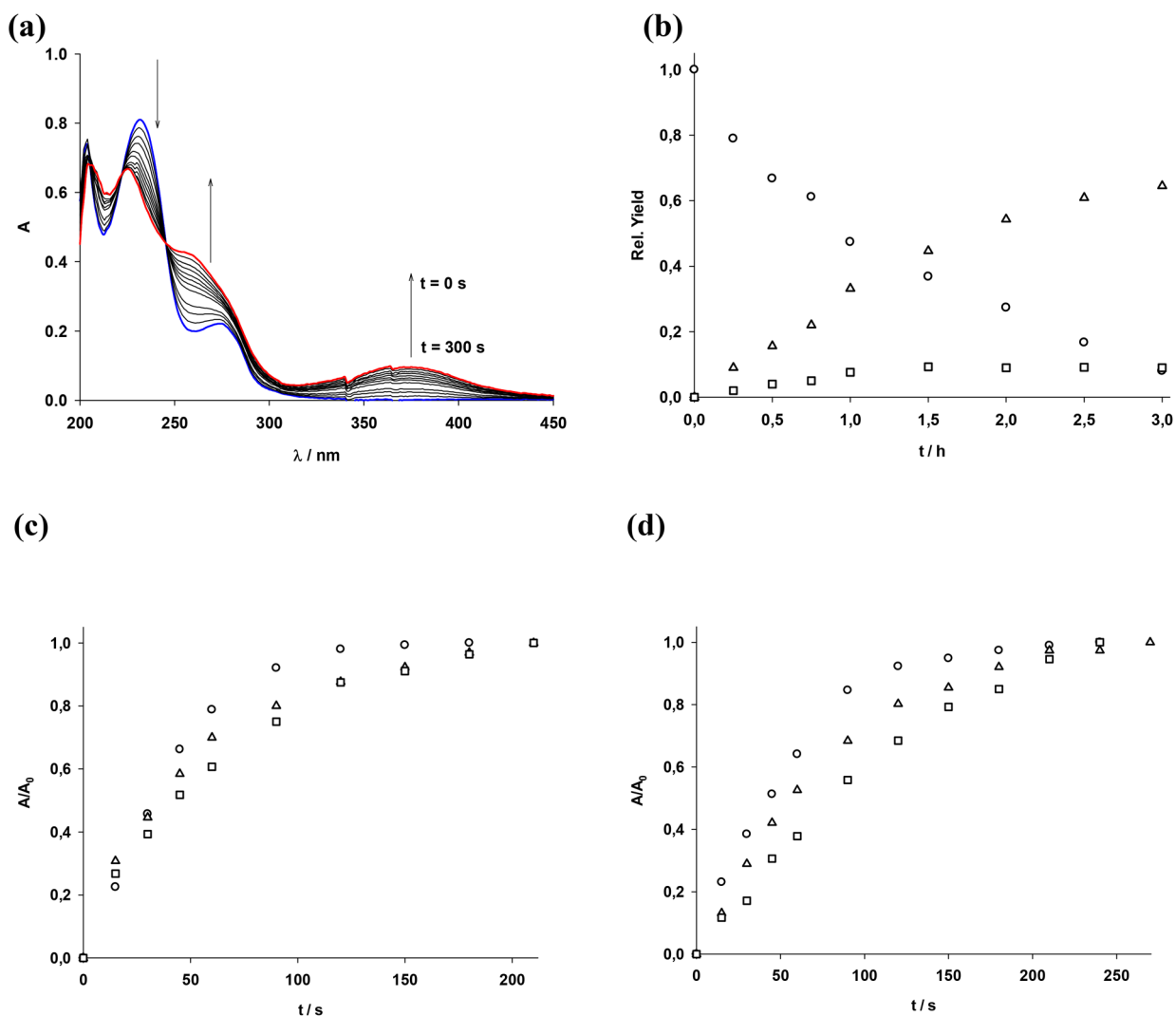
(a)

(b)

(c)

(d)

Figure 2. (a) UV−vis spectral change vs time of **1** in SDS 0.10 M in water. Blue line: initial time; red line: 300 s. (b) Relative yield profile vs time of **1** in MeOH: ester **1** (circles); benzophenone **1a** (triangles); phenol **1b** (square). (c) Relative absorbance at 375 nm (A/A_∞) of formation of **7a** in cyclohexane (circles); 0.10 M SDS solution (triangles); 0.10 M Brij-P35 solution (square). (d) Relative absorbance at 355 nm (A/A_∞) of formation of **4a** in cyclohexane (circles); 0.10 M SDS solution (triangles); 0.10 M Brij-P35 solution (square).

at 290, 340, 400, and 720 nm were observed in the transient spectra. According to the data reported in the literature, we attributed the bands located at 290 and 400 nm to the *p*-methoxyphenoxyl radical, while those bands centered at 340 and 720 nm were attributed to the cyclohexadienone transient.[20] Two consecutive pathways from the singlet excited state of ester **1** are involved in the formation of both transients after the pulse (266 nm): (i) homolytic fragmentation of the C−O bond of the ester group affording *p*-methoxyphenoxy and benzoyloxy radical species in the solvent cage (intermediates **A** and **B**, respectively, in Scheme 4) and then (ii) coupling of both radical species to give the 4-methoxy-2-benzoylcyclohexadienone intermediate (**C** in Scheme 4). Also, in Figure 5c,d are reported the transient absorption spectra of compounds **6** and **2** in acetonitrile after laser pulse (266 nm). Two characteristic bands located around 340 and 400 nm are observed which were assigned to substituted 2-benzoylcyclohexadienone and substituted phe-noxy radical intermediates, respectively. Note that y similar results are obtained for the other aryl benzoates studied (see Figure S9, Supporting Information).

The decay traces of the transient signal assigned to 4-substituted phenoxyl radicals were also measured at 400 nm in N_2-saturated cyclohexane and acetonitrile solutions (after a laser pulse at 266 nm). The experiment was done with the aim of determining both the rate constants of radical out-of-cage escape (k_E) and *ortho* coupling reaction (k_R) (see Scheme 4). Some selected examples of the decay traces are shown in Figure 6. The decay traces of 4-substituted phenoxyl radicals show biexpo-nential decay fitting with r^2 values >0.998 independent of the solvent used. Two half lifetime values were obtained from the nonlinear fittings, τ_E and τ_R: the short lifetime (τ_R) was assigned to an in-cage coupling process, while the large lifetime (τ_E) was assigned to the phenoxyl radical out-of-cage process by comparison with previously reported data regarding thiyl radicals.[20e,21] This biexponential behavior can be interpreted considering the two competitive pathways the 4-substituted phenoxyl radical can undergo, viz. out-of-cage escape and in-cage coupling pathways (see Scheme 4). This behavior can be described according to eq 4 where ArO• represents the
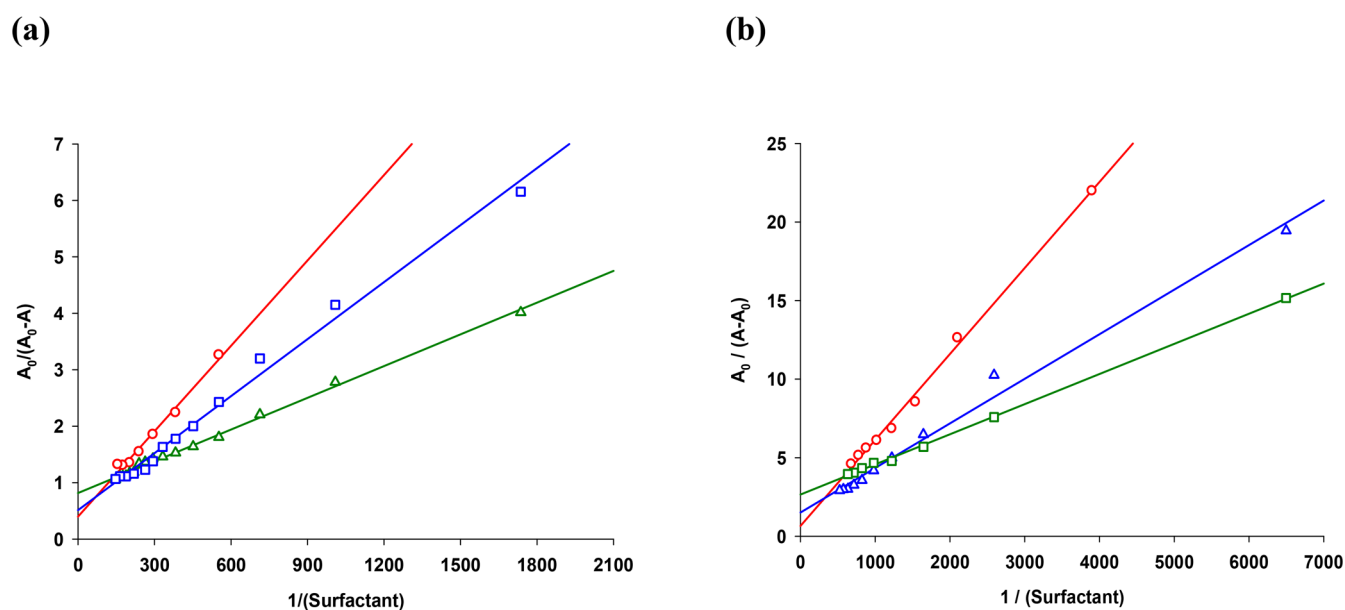
(a)

(b)

Figure 3. Reciprocal plotting ($(A_0/(A - A_0)$ vs concentration of surfactants) in water at room temperature: (a) SDS (circles: **2**; squares: **4**; triangles: **7**) and (b) Brij-P35 (circles: **2**; squares: **4**; triangles: **1**). In all of the linear fitting regressions: $r^2 > 0.99$.

Table 3. Binding Constant (K_b) in Water of Surfactants (SDS and Brij-P35) and Aryl Benzoates

aryl benzoates	K_b (M^{-1})							
	1	2	3	4	5	6	7	8
SDS	1402	80	127	539	42	10	18	74
Brij-P35	1398	581	69	423	63	26	1394	181
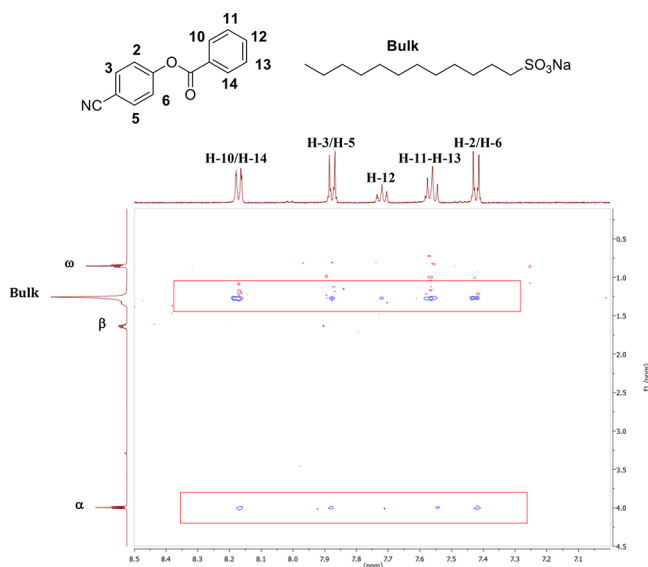
Figure 4. 2D NOESY contour plot of a solution of SDS (7 mM) and **7** (10 mM) in D$_2$O at room temperature.

substituted phenoxy radical and PhCO$^\bullet$ represents the benzoyl radical.

$$-\frac{d[\text{ArO}^\bullet]}{dt} = k_E[\text{ArO}^\bullet] + k_R \text{ArO}^\bullet[\text{Ph\.CO}] \qquad (4)$$

The out-of-cage escape of the substituted phenoxy radical is a unimolecular pathway. Therefore, the rate constant (k_E) of this process can be calculated from the reciprocal of the lifetime, $k_E = 1/\tau_E$ (see Table 4). The in-cage coupling rate constants (k_R) were obtained by plotting the reciprocal of the concentration of the substituted phenoxy radicals against time, and excellent linear correlations were observed (see Figure S11, Supporting Information, for the linear correlations). Then, after application of a linear regression fitting the in-cage coupling rate constants (k_R) were obtained from the slopes, and these data are also shown in Table 4. As can be seen in Table 4, it is apparent that the out-of-cage rate constants (k_E) for the unimolecular escape process of 4-substituted phenoxyl radicals are quite similar in all the solvents studied ($(1.5-8.3) \times 10^5$ s^{-1}) and somewhat independent of the substituent. On the other hand, the bimolecular in-cage coupling of 4-substituted phenoxyl and benzoyl radicals was found to be a second-order rate constant (k_R) of 10^9-10^{10} M$^{-1}\cdot$s^{-1} in N$_2$-saturated solvents with no significant substituent effect associated to it.

A similar spectroscopic analysis was carried out with aryl benzoates in aqueous SDS (0.10 M) solutions after irradiation with a pulse at 266 nm. Two characteristic bands (340−360 and 400 nm) are observed in the transient absorption spectra, and 4-substituted phenoxyl radicals showed second-order kinetic decay traces. The in-cage coupling rate constants (k_R) were obtained by plotting the reciprocal of the concentration of the 4-substituted phenoxyl radicals against time, and after applying a linear regression fitting, the rate constants (k_R) were obtained from the slopes (see Table 4). No significant substituent effect on the rate constants (k_R) was observed when the solvent was a micellar solution (SDS 0.10 M), which gave a trend similar to that observed in homogeneous media.

Because phenyl benzoate (**5**) has no substituent in the *para* position, two possible *o*- and *p*-benzoylcyclohexadienone regioisomers can be proposed (see Scheme 5). Therefore, we have recorded the transient absorption spectra and transient decay traces of compound **5** in different N$_2$-saturated solvents with a laser pulse at 266 nm systematically. Figure 7a shows both the transient absorption spectra and decay trace recorded at 400 nm in MeCN. The band located at 400 nm in the transient absorption spectra was assigned to the phenoxyl radical, while
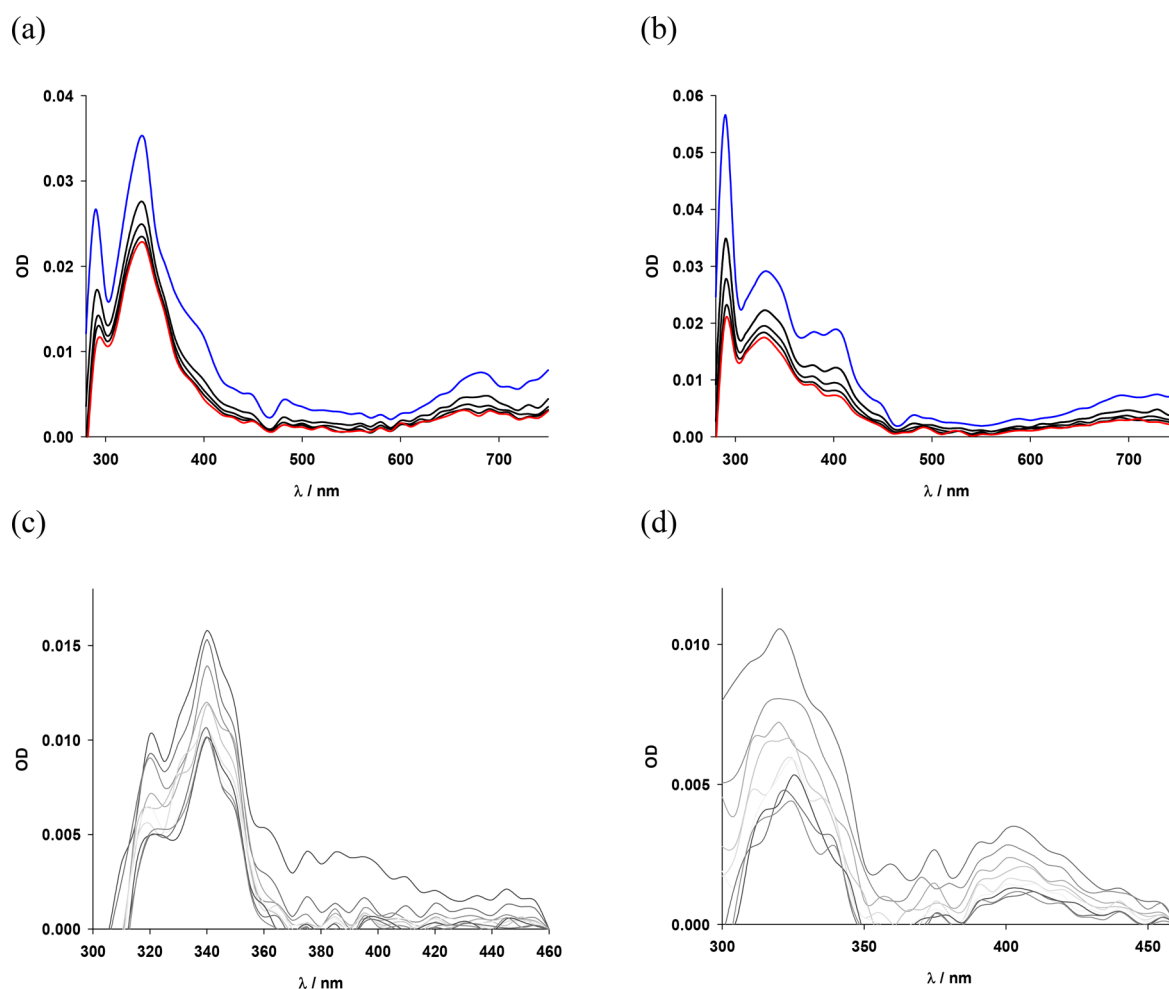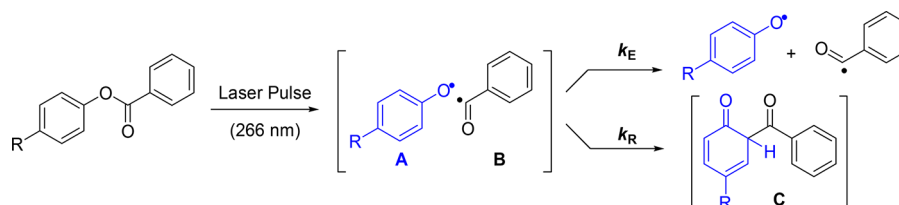
(a)

(b)

(c)

(d)

Figure 5. Transient absorption spectra obtained after a laser pulse ($100\ \mu s$; λ_{exc}: 266 nm) of solutions (5.1×10^{-4} M) of (a) **1** in cyclohexane, (b) **1** in acetonitrile, (c) **6** in acetonitrile, and (d) **2** in acetonitrile under nitrogen atmosphere.

Scheme 4. Formation of Transient Species after the Laser Pulse (266 nm)

the large structured band located between 330 and 385 nm was assigned to *o*-benzoylcyclohexadienone and *p*-benzoylcyclohexadienone transients (see Scheme 5).

On the other hand, Figure 7b shows the decay trace of phenoxyl radical measured at 400 nm in N_2-saturated acetonitrile solution after the laser pulse (266 nm). Biexponential decay was observed after a nonlinear fitting. This biexponential behavior can be interpreted considering the competitive pathways the phenoxyl radical can take viz. out-of-cage escape and *ortho* and *para* in-cage coupling pathways (see Scheme 5). The rate constant (k_E) of the out-of-cage escape pathway was calculated from the reciprocal of the lifetime, $k_E = 1/\tau_E$. The rate constants thus obtained are shown in Table 5. In addition, the *ortho* and *para* in-cage coupling constants, k_{ortho} and k_{para}, were obtained by plotting the reciprocal of the concentration of the phenoxy radical against time, and two nice

linear correlations were observed (see Figure S12, Supporting Information, for the linear correlations). Then, after a linear regression fitting was applied to the linear correlations, the in-cage coupling constants were obtained from the slopes, and these data are also shown in Table 5. No significant solvent effect on the rate constants was observed. However, the in-cage *para*-coupling pathway is rather lower than the *ortho*-coupling pathway.

■ DISCUSSION

As it was described above, direct irradiation (254 nm) of aryl benzoates in homogeneous media (cyclohexane, MeCN and MeOH) as well as in micro heterogeneous media (SDS and Brij-P35 aqueous solutions) under N_2 atmosphere took place efficiently (see Figures 1 and 2). During the irradiation of aryl benzoates, a noticeable selectivity in favor of the benzophenone

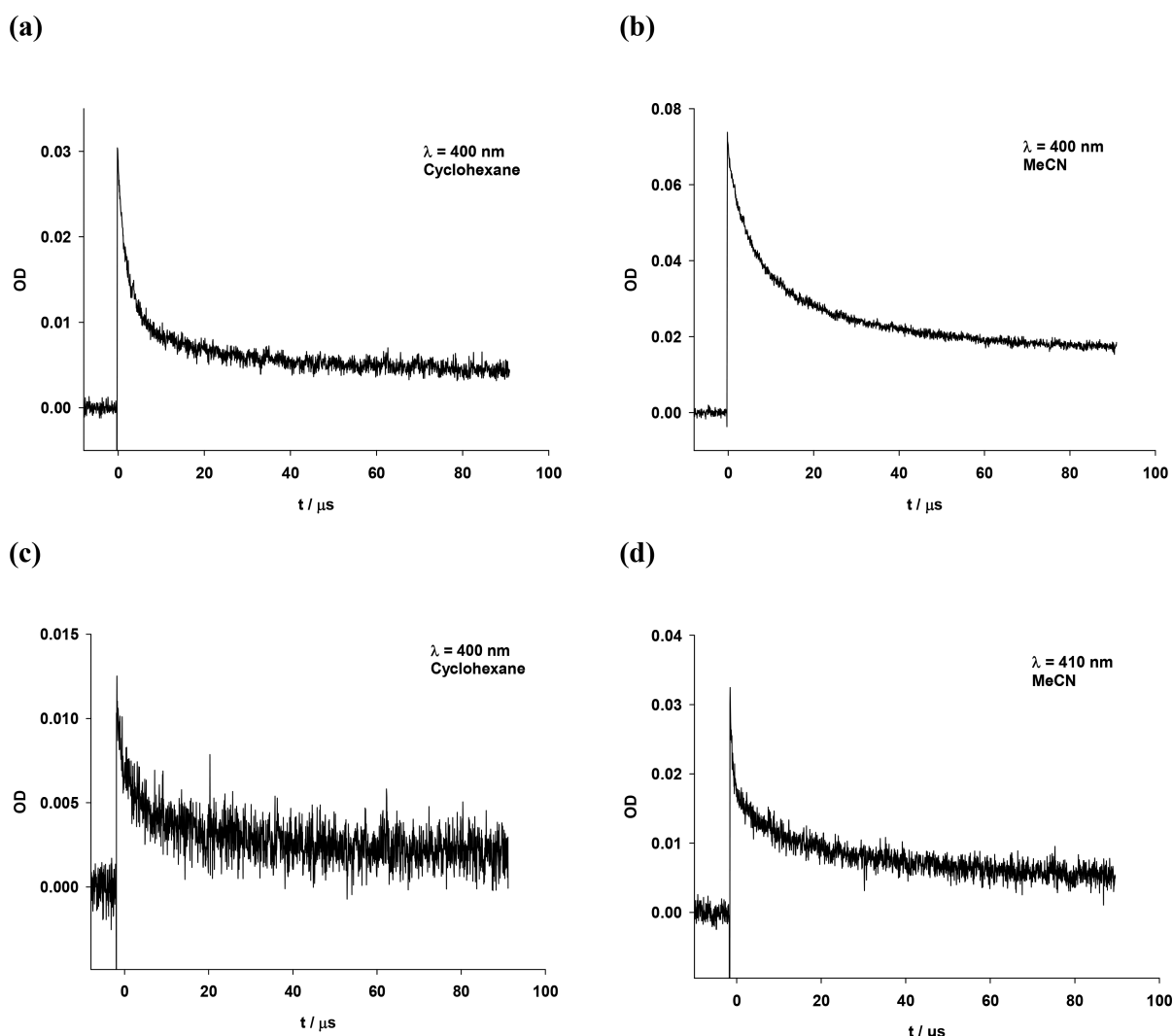**Figure 6.** Decay traces of 4-substituted phenoxyl radical recorded at 400 nm after the laser pulse (λ_{exc}: 266 nm) of solutions (5.1×10^{-4} M) of (a) 4-methoxyphenyl benzoate (**1**) in cyclohexane; (b) 4-methoxyphenyl benzoate (**1**) in acetonitrile; (c) 4-*tert*-butylphenyl benzoate (**4**) in cyclohexane; (d) 4-phenoxyphenyl benzoate (**2**) in acetonitrile under N$_2$ atmosphere.

Table 4. Out-of-Cage (k_E) and in-Cage Coupling (k_R) Rate Constants of 4-Substituted Phenoxyl Radicals Measured by Laser Flash Photolysis (266 nm) in Different Solvents under N$_2$ Atmosphere[a]

				Rate constants			
		MeCN		MeOH		Cyclohexane	SDS (0.10 M)
R	$k_{EX}10^{-5}$ / s^{-1}	$k_{RX}10^{-9}$ / M^{-1}.s^{-1}	$k_{EX}10^{-5}$ / s^{-1}	$k_{RX}10^{-9}$ / M^{-1}.s^{-1}	$k_{EX}10^{-5}$ / s^{-1}	$k_{RX}10^{-9}$ / M^{-1}.s^{-1}	$k_{RX}10^{-9}$ / M^{-1}.s^{-1}
OMe (**1**)	2.2±0.1	5.5±0.1	2.8±0.1	15±1	4.5±0.1	8.9±0.1	3.9±0.1
OPh (**2**)	8.3±0.2	14±1	1.0±0.2	24±1	2.2±0.2	46±1	25±1
Me (**3**)	3.0±0.1	1.4±0.1	6.7±0.1	1.7±0.1	2.5±0.1	7.3±0.1	3.0±0.1
t-Bu (**4**)	1.5±0.1	28±1	3.4±0.1	12±1	3.4±0.1	3.4±0.1	26±1
Ph (**6**)	5.0±0.2	4.6±0.1	1.0±0.2	6.1±0.1	Insoluble		1.2±0.1
CN (**7**)	4.8±0.2	9.5±0.1	2.3±0.2	9.9±0.1	1.3±0.2	36±1	17±1

[a]Concentration of aryl benzoates: 5.0×10^{-4} M.

derivatives was observed in micellar media. In this case, the formation of the corresponding substituted phenols was lower than 2% because of the confined hydrophobic core of the micelle (compare the data shown in Tables 1 and 2). The reaction mechanism depicted in Scheme 6 was sustained by the results obtained under steady-state conditions and laser flash photolysis experiments. When aryl benzoates are irradiated at 254 nm, the population of the singlet state is achieved efficiently. This excited state is the photoreactive state of the photoreaction as reported in the literature.[5] Two pathways are involved in the deactivation

Scheme 5. Formation of Transient Species after the Laser Pulse (266 nm) from Phenyl Benzoate
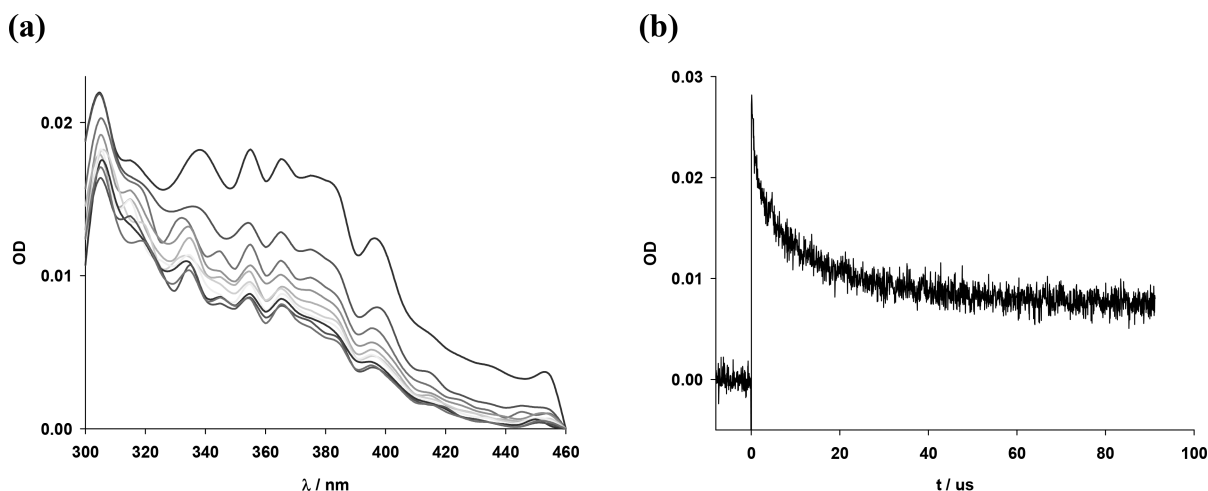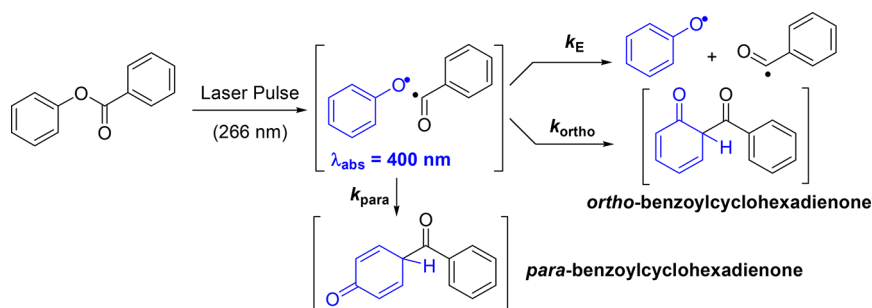

Figure 7. (a) Transient absorption spectra of phenyl benzoate (**5**) recorded in N_2-saturated acetonitrile solution (5.1×10^{-4} M) and (b) decay trace of phenoxyl radical recorded at 400 nm after the laser pulse (100 μs; λ_{exc}: 266 nm) of N_2-saturated acetonitrile solution (5.1×10^{-4} M) of phenyl benzoate (**5**).

Table 5. Out-of-Cage (k_E) and in-Cage Coupling (k_{ortho} and k_{para}) Rate Constants of Phenoxyl Radicals Measured by Laser Flash Photolysis (266 nm) in Different Solvents under N_2 Atmosphere[a]

|	rate constants		
solvents	$k_E \times 10^{-5}$ (s^{-1})	$k_{ortho} \times 10^{-9}$ ($M^{-1} \cdot s^{-1}$)	k_{para} tme x10^{-9} ($M^{-1} \cdot s^{-1}$
cyclohexane	4.8 ± 0.1	8.7 ± 0.1	4.1 ± 0.1
MeCN	4.8 ± 0.1	8.4 ± 0.1	3.2 ± 0.1
MeOH	3.1 ± 0.1	2.7 ± 0.1	1.4 ± 0.1
SDS (0.10 M)		5.5 ± 0.2	1.5 ± 0.2

[a]Concentration of phenyl benzoates: 5.0×10^{-4} M.

of the singlet state: (i) homolytic fragmentation of the C−O bond (path a; Scheme 6) affording aryl phenoxy (ArO•) and benzoyl (PhCO•) radicals that evolve to 5-substituted 2-hydroxybenzophenone and 4-substituted phenol and (ii) photophysical deactivation (k_d; Scheme 3) of the singlet state involving fluorescence emission and internal conversion pathways that give the aryl benzoates in their ground state. In the case of ester **8**, intersystem crossing pathway must be considered as a process involved in the physical deactivation pathway estimating a ϕ_T value around 0.50.[14,15] Irradiation of aryl benzoates in N_2-saturated solutions with a laser pulse (λ_{exc} = 266 nm) gave the transient absorption of 4-substituted phenoxyl radical and 5-substituted 2-benzoylcyclohexadienone, and these transients were formed immediately at 10 μs after the incident light (see,

Scheme 6. Reaction Mechanism for the Irradiation of Aryl Benzoates with λ_{exc} = 254 nm

J
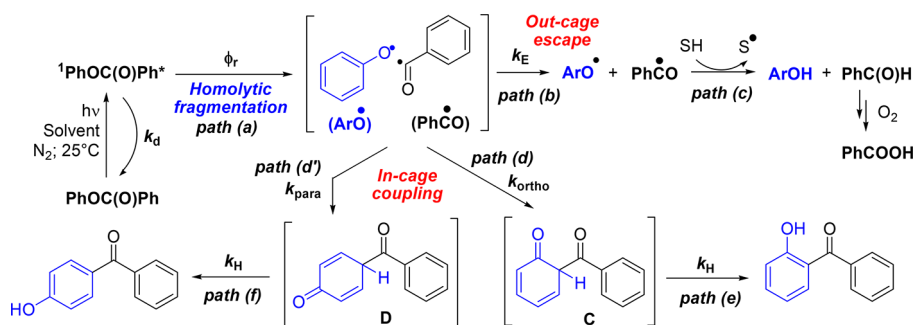
Scheme 7. Proposed Reaction Mechanism for Direct Irradiation of Phenyl Benzoate (5)
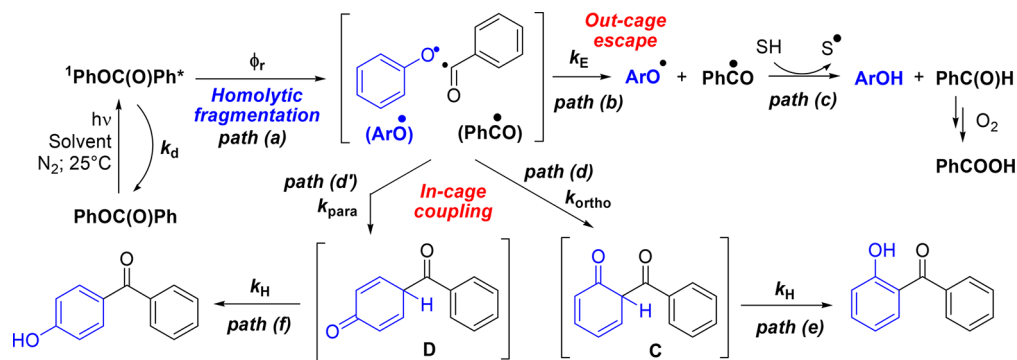
for example, Figure 5 for compounds **1**, **2**, and **6**), demonstrating that C−O homolytic fragmentation (path a in Scheme 6) and in-cage coupling pathway (path d in Scheme 6) occurred efficiently.

The decay traces of the phenoxyl radical transients were obtained at 400 nm in homogeneous media under inert atmosphere, and biexponential decay was observed. Second-order kinetics (k_R) of 10^9–10^{10} $M^{-1}\cdot s^{-1}$ were obtained (see Table 4 and Figure 6) and were attributed to the in-cage coupling of the substituted phenoxy radical and benzoyl radical (path d in Scheme 6) providing the substituted 2-benzoylcyclohexadienone intermediates **C**. These last intermediates, i.e., intermediates **C**, are long-lived species showing lifetime values higher than 200 μs. The [1;3]-hydrogen migration and aromatization reaction pathway (path e in Scheme 6) were estimated to occur with first-order kinetics (k_H) lower than 5×10^3 s^{-1}, providing the substituted 2-hydroxybenzophenone derivatives as the main photoproducts (see Table 1). On the other hand, first-order kinetics (k_E) of 10^5 s^{-1} were also obtained (see Table 4) which were assigned to the escape of the phenoxy radical from the solvent cage (path b in Scheme 6) that in turn evolved to the 4-substituted phenol by abstraction of hydrogen from the reaction solvent (path c in Scheme 6; SH: solvent).

Second-order rate constants (k_R) in the range of 10^9–10^{10} $M^{-1}\cdot s^{-1}$ were obtained (see Table 4) from the fitting analysis of the decay traces of the phenoxyl radicals measured at 400 nm in micellar media (SDS and Brij-P35) under N_2 atmosphere. These values describe the in-cage coupling within the core of the micelle of the substituted phenoxy radical $(ArO^{\bullet})$ and benzoyl radical $(PhC(O)^{\bullet})$ (see path d in Scheme 6). This pathway afforded the substituted 2-benzoylcyclohexadienone intermediates **C**, also formed within the hydrophobic core of the micelle, that evolved through a [1;3]-hydrogen migration and aromatization reactions to substituted 2-hydroxybenzophenone. Because intermediates **C** are also long-lived species in micellar media $(\tau > 200\ \mu s)$, the rate constants k_H were estimated to be lower than 5×10^3 s^{-1} as observed in homogeneous media.

It is worth mentioning that the only photoproducts detected in micellar media were the 2-hydroxybenzophenone derivatives **1a**−**8a** formed with chemical yields up to 95% (see Table 2), and the yields of the substituted phenols were lower than 5%. Therefore, we suggest that the escape of the phenoxy radical from the hydrophobic core of the micelle (path b in Scheme 6) is not a productive pathway. The decay traces of phenoxy radicals in micellar media did not show biexponential decay traces as observed in homogeneous media but second-order kinetics, which is in agreement with the in-cage coupling pathway (path d in Scheme 6).

Additional comments about the irradiation of phenyl benzoate (**5**) in homogeneous and micellar media are needed. The results obtained under steady-state conditions and time-resolved spectroscopy on phenyl benzoate led us to advance the different reaction pathways depicted in Scheme 7. Irradiation of phenyl benzoate populated the singlet excited state efficiently, and competitive physical deactivation (k_d) and homolytic fragmentation (path a in Scheme 7) pathways occurred.

After fragmentation phenoxy and benzoyl radical species were formed in the solvent cage, escape of the radical species from the solvent cage (path b) and hydrogen abstraction from the solvent (path c) gave the conventional products. Laser flash photolysis experiments provided rate constants (k_E) in cyclohexane, MeCN, and MeOH (see Table 5) following the decay trace of the phenoxy radical at 400 nm. No escape of the radical species was detected in micellar solution. Because phenyl benzoate has no substituent in the *para* position, two possible *o*- and *p*-benzoylcyclohexadienone regioisomers viz. intermediates **C** and **D** were formed through the in-cage coupling of the radical species (path d and path e in Scheme 7). Both intermediates **C** and **D** were observed in the absorption transient spectra (see Figure 7) with characteristic bands located in the range of 340−380 nm. Besides, the k_{ortho} and k_{para} values on the order of 10^9 $M^{-1}\cdot s^{-1}$ belonging to in-cage coupling pathways (paths d and d′ in Scheme 7) implied that the coupling reaction occurred efficiently in all the solvents studied. Then intermediates **C** and **D** formed in the solvent cage evolved to the regioisomers 2-hydroxybenzophenone and 4-hydroxybenzophenone through the sequence [1,3]-hydrogen migration and aromatization pathways (path e and path f in Scheme 7). Again, intermediates **C** and **D** showed lifetimes higher than 200 μs, and the rate constant k_H was estimated to be lower than 10^3 s^{-1}. These photoproducts were formed with 30−60% yields together with the corresponding phenol in homogeneous media (see Table 1), while in micellar solution they were formed in up to 95% yield and no phenol was detected in the micellar reaction mixture.

■ CONCLUSIONS

The photochemical reaction of aryl benzoates examined in this paper takes place efficiently in homogeneous and micellar media. High selectivity in the formation of the 5-substituted 2-hydroxybenzophenone derivatives was observed in micellar media, providing these photoproducts in yields up to 95% without the formation of the corresponding phenols. Location of the aryl benzoates with 2D NOESY NMR spectroscopy in the shell or in the hydrophobic core of the micelle and measurement of the binding constants (K_b) between the benzoates and the surfactants account for the selective behavior observed where

diffusion of the radical species from the micelle is inhibited. On the other hand, benzophenone derivatives, as the main photoproducts, and the *para*-substituted phenols were formed when the irradiations were carried out in homogeneous media such as cyclohexane, MeCN, and MeOH, but no selectivity was observed.

Laser flash photolysis led us to characterize two intermediates viz. the substituted phenoxy radical and the 5-substituted 2-benzoylcyclohexadienone transients. These intermediates were formed in the cage solvent within 10 μs after the laser pulse. In addition, the phenoxy radical escapes from the solvent cage with first-order rate constants (k_E) of 10^5 s^{-1} that in turn evolve to the corresponding phenols by hydrogen abstraction from the reaction solvent (see Schemes 6 and 7). The kinetic parameters (k_R) for in-cage coupling pathways of the radical species viz. substituted phenoxy and benzoyl radicals were also measured in all of the solvents studied, providing the corresponding 5-substituted 2-benzoylcyclohexadienone intermediates (intermediate **C** in Scheme 6 and intermediates **C** and **D** in Scheme 7). These species which are formed in the solvent cage evolved to the regioisomeric 5-substituted 2-hydroxybenzophenone derivatives through the sequence [1;3]-hydrogen migration and aromatization pathways (path e in Scheme 6 and path f in Scheme 7). Because these intermediates showed lifetimes higher than 200 μs, the rate constants k_H were estimated to be lower than 10^3 s^{-1} in all of the solvents studied.

Finally, the finding that the selectivity observed in the photo-Fries rearrangement of some aryl benzoates in green and sustainable micellar media gives 5-substituted-2-hydroxybenzophenone derivatives in yields up to 95% could be applied in the preparation of a new wide variety of substituted 2-hydroxybenzophenoe derivatives.

■ EXPERIMENTAL SECTION

Materials and Equipment. *Para*-substituted phenols, benzoyl chloride, pyridine, sodium dodecyl sulfonate, and Brij-P35 were obtained from commercial sources. Spectroscopic grade solvents were used as received. Pyridine was distilled and stored over KOH pellets. Melting points were determined with a Fisher Jones apparatus and are not corrected. ^{1}H and ^{13}C NMR spectra were recorded in CDCl$_3$ on a 300 MHz spectrometer; chemical shifts (δ) are reported in part per million (ppm), relative to signal of tetramethylsilane, used as internal standard. 2D NOESY spectra were recorded in D$_2$O on a 500 MHz spectrometer, using a NOESY-ph pulse sequence with a 600 ms mixing time and a recovery delay of 1.5 s. 2K data points were collected for 512 increments of 16 scans, using TPPI f1quadrature detection; chemical shifts (δ) are reported in part per million (ppm), relative to the signal of trimethylsilylpropionic acid, used as internal standard. Coupling constant (J) values are given in hertz. The measurements were carried out using standard pulse sequences. GC analysis was carried out on a Hewlett-Packard 5890 gas chromatograph using an Ultra 2 capillary chromatographic column. The chromatograms were recorded with the following program: initial temperature: 100 °C, 2 min; gradient rate: 10 °C.min^{-1}; final temperature: 250 °C, 10 min. The UV−vis spectra were measured with a Shimadzu UV-1203 spectrophotometer using two-faced stoppered quartz cuvettes (1 mm × 1 mm) at 298 K.

Determination of the Binding Constants (K_b) of Phenyl Benzoates in Micellar Media. Solutions of phenyl benzoates were prepared in deionized water (Milli-Q), and their concentrations varied between 5.5 × 10^{-5} M and 1.0 × 10^{-4} M. An aliquot (2 mL) of the phenyl benzoate solution was placed in a fluorescence-stoppered quartz cuvette provided with a stirring bar, and the UV−vis spectrum was recorded. The initial absorbance value at the maximum absorption wavelength (A_0) was read. Subsequently, aliquots of concentrated surfactant solution (10 μL) were added. The UV−vis spectra were registered, recording for each solution the A value at the maximum absorption wavelength. After each addition of surfactant, the solution was stirred for 20 min before measuring the absorbance. With the values of A_0 and A in hand, the values of ($A_0/(A − A_0)$) versus the reciprocal of the concentration of the micellar surfactant were plotted, and the data were fitted with a linear regression program. The K_b values were obtained by calculating the ratio of the slope and the origin.

Laser Flash Photolysis. The laser pulse photolysis apparatus consisted of a Flash lamp-pumped Q-switched SpitLight-100 Nd:YAG laser from InnoLas used at the fourth harmonic of its fundamental wavelength. The LP920-K monitor system (supplied by Edinburgh Instruments), arranged in a cross-beam configuration, consisted of a high-intensity 450 W ozone free Xe arc lamp (operating in pulsed wave), a Czerny-Turner with triple grating turret monochromator, and a five-stage dynode photomultiplier. The signals were captured by means of a Tektronix TDS 3012C digital phosphor oscilloscope, and the data were processed with the L900 software supplied by Edinburgh Instruments. The solutions to be analyzed were placed in a fluorescence cuvette (d = 10 mm).

Synthesis of Phenyl Benzoates 1−8. To a solution of the substituted phenols (0.010 mol) in pyridine (10 mL) cooled in an ice bath was added benzoyl chloride (0.012 mol) dropwise over 10 min with stirring. Subsequently, the reaction mixture was kept under stirring for 60 min. After total consumption of the starting material was confirmed by TLC, the reaction mixture was extracted with dichloromethane (10 mL) and washed with a solution of diluted HCl (10 mL). The organic phase was then washed with water, dried on Na$_2$SO$_4$, filtrated, and evaporated under pressure. The phenyl benzoates were purified from the solid residue by recrystallization using ethanol−water mixtures to give the corresponding phenyl benzoates in excellent yields (>90%). The aryl benzoates **1−8** were characterized by comparing the physical constant (mp) and spectroscopic data (^{1}H NMR and ^{13}C NMR) with the ones reported in the literature.

Photoirradiation of Phenyl Benzoates in Homogeneous Media. A stock solution of a given benzoate (**1−8**, 0.106 mmol in 200 mL cyclohexane) was placed in a stoppered Erlenmeyer quartz flask and degassed with argon for 30 min. The flask was placed in a homemade optical bench provided with the possibility to use four or eight lamps. The solution was stirred during the entire irradiation. Irradiations with λ_{exc} = 254 nm were carried out with four germicide lamps (Philips, each of 20 W, purchased in Argentina). The reaction progress was monitored by TLC [eluent: hexane−ethyl acetate (8:2 v/v); spots were visualized with UV light (254 and 366 nm)] and by GC analysis (Ultra 2 capillary column). When the conversion of the starting material was higher than 90%, the photolyzed solution was carefully evaporated to dryness under reduced pressure. The yellowish solid residue obtained was purified by silica gel column chromatography (eluent: hexane 100% followed by hexane−ethyl acetate mixtures). From the eluted fractions, the photoproducts were isolated and characterized by means of physical and spectroscopic methods.

Photoirradiations of Phenyl Benzoates in Micellar Media. Stock solutions of surfactants in deionized water (SDS 0.10 M and Brij-P35 0.05 M) were freshly prepared before each experiment. The aryl benzoate (5 mg) was placed in a stoppered quartz cell provided with a stirring bar (3 mL), and the surfactant stock solution (2 mL) was added. Then the solution was vigorously stirred for 1 h and degassed with argon for 20 min. The quartz cell was placed in a homemade optical bench provided with two germicide lamps (each of 20 W). The progress of the photoreaction was monitored by two different methods: (i) UV−vis spectroscopy and GC analysis (Ultra 2 capillary column). The conversion of the benzoates was kept below 20% to avoid secondary reactions and the formation of byproducts. Previous to the injection into the GC apparatus, the micellar solutions were treated as follows. The photolyzed solutions were diluted with 2 mL of an aqueous solution of NaCl and then extracted with ethyl acetate (3 × 2 mL) while the system was carefully shaken to avoid the formation of emulsions. The organic layer was separated, dried over Na$_2$SO$_4$, and evaporated to dryness under vacuum. The yellowish solid residue was diluted in dichloromethane (2.00 mL), and this solution was injected into the GC

for chromatographic analysis. The products were characterized by comparison of physical constant (mp) and spectroscopic data (^{1}H NMR and ^{13}C NMR) with those reported in the literature.

p-Methoxyphenyl Benzoate (1). White needles (2.24 g; 98%). Mp: 89−90 °C (lit.[22] mp 87−88 °C). ^{1}H NMR (300 MHz, CDCl$_3$): δ 8.23 (d, *J* = 8.6 Hz, *J* = 1.4 Hz, 2H), 7.66 (dd, *J* = 8.6 Hz, *J* = 1.3 Hz, 2H), 7.53 (t, *J* = 7.8 Hz, *J* = 1.1 Hz, 1H), 7.17 (d, *J* = 9.4 Hz, 2H), 6.97 (d, *J* = 9.4 Hz, 2H), 3.85 (s, 3H). ^{13}C{^{1}H} NMR (75 MHz, CDCl$_3$): δ 165.4, 157.2, 144.3, 133.4, 130.0, 129.6, 128.4, 122.3, 114.4, 55.5.

p-Phenoxyphenyl Benzoate (2). White plates (2.84 g; 98%). Mp: 100−101 °C.[23] ^{1}H NMR (300 MHz, CDCl$_3$): δ 8.24 (d, *J* = 7.1, 1.0 Hz, 2H), 7.67 (t, *J* = 7.7 Hz, 1H), 7.55 (t, *J* = 7.9 Hz, 2H), 7.39 (t, *J* = 8.4 Hz, 2H), 7.21 (d, *J* = 8.9 Hz, 2H), 7.18−7.04 (m, 5 H). ^{13}C{^{1}H} NMR (75 MHz, CDCl$_3$): δ 165.2, 157.1, 146.2, 133.5, 130.1, 129.7, 129.4, 128.5, 123.5, 122.7, 119.6, 118.7.

p-Methylphenyl Benzoate (3). White needles (2.02 g; 95%). Mp: 71 °C (lit.[24] mp 72 °C). ^{1}H NMR (300 MHz, CDCl$_3$): δ 8.24 (d, *J* = 8.2 Hz, *J* = 1.4 Hz, 2H), 7.65 (dd, *J* = 7.4 Hz, *J* = 1.2 Hz, 2H), 7.54 (t, *J* = 7.8 Hz, *J* = 1.2 Hz, 1H), 7.25 (d, *J* = 8.3 Hz, 2H), 7.13 (d, *J* = 8.5 Hz, 2H), 2.41 (s, 3H). ^{13}C{^{1}H} NMR (75 MHz, CDCl$_3$): δ 165.3, 148.6, 135.4, 133.4, 130.1, 129.6, 129.9, 128.4, 121.3, 20.8.

p-tert-Butylphenyl Benzoate (4). White plates (2.44 g; 96%). Mp: 83−84 °C (lit.[25] mp 82−83 °C). ^{1}H NMR (300 MHz, CDCl$_3$): δ 8.23 (dd, *J* = 7.9, 1.6 Hz, 2H), 7.66 (t, *J* = 7.4 Hz, 2H), 7.55 (t, *J* = 8.7 Hz, 1H), 7.47 (d, *J* = 8.7 Hz, 2H), 7.17 (d, *J* = 8.7 Hz, 2H), 1.35 (s, 9H). ^{13}C{^{1}H} NMR (75 MHz, CDCl$_3$): δ 165.2, 148.6, 148.5, 133.4, 130.0, 129.6, 128.4, 126.3, 120.9, 34.4, 31.6.

Phenyl Benzoate (5). White solid (1.94 g; 98%). Mp: 69−70 °C (lit.[6a] mp 67−69 °C). ^{1}H NMR (300 MHz, CDCl$_3$): δ 8.25 (d, *J* = 7.4 Hz, 2H), 7.67 (t, *J* = 7.6 Hz, 1H), 7.55 (t, *J* = 8.1 Hz, 2H), 7.45 (t, *J* = 8.3, 7.8 Hz, 2H), 7.32 (t, *J* = 8.1, 7.2 Hz, 1H), 7.24 (d, *J* = 7.2 Hz, 2H). ^{13}C{^{1}H} NMR (75 MHz, CDCl$_3$): δ 165.1, 150.9, 133.5, 130.1, 129.5, 129.4, 128.5, 125.8, 121.6.

p-Phenylphenyl Benzoate (6). White needles (2.52 g; 92%). Mp: 150−151 °C.[23] ^{1}H NMR (300 MHz, CDCl$_3$): δ 8.20 (d, *J* = 8.2, 1.2 Hz, 2H), 7.72−7.61 (m, 5H), 7.57 (t, *J* = 7.9 Hz, 2H), 7.49 (t, *J* = 7.8 Hz, 2H), 7.41 (d, *J* = 7.2 Hz, 1H), 7.33 (d, *J* = 8.6 Hz, 2H). ^{13}C{^{1}H} NMR (75 MHz, CDCl$_3$): δ 165.1, 150.3, 140.3, 138.9, 133.5, 130.1, 129.4, 128.7, 128.5, 128.1, 127.3, 127.0, 121.9.

p-Cyanophenyl Benzoate (7). White solid (2.01 g; 90%). Mp: 94−95 °C (lit.[26] mp 91−92 °C). ^{1}H NMR (300 MHz, CDCl$_3$): δ: 8.22 (d, *J* = 8.4 Hz, 2H), 7.74 (d, *J* = 7,64 Hz 2H), 7.70 (t, *J* = 7.0, 7.64 Hz, 2H) 7.56 (t, *J* = 7.6 Hz, 2H), 7.4 (d, *J* = 8.4 Hz, 2H). ^{13}C{^{1}H} NMR (75 MHz, CDCl$_3$) δ: 164.2, 154.1, 134.0, 133.6, 130.1, 128.6, 128.5, 122.8, 118.2, 109.7.

p-Nitrophenyl Benzoate (8). Pale yellow needles (2.21 g; 91%). Mp: 144−145 °C (lit.[27] mp 142−144 °C). ^{1}H NMR (300 MHz, CDCl$_3$) δ: 8.34 (d, *J* = 9.1 Hz, 2H), 8.23 (dd, *J* = 7.6, 1.3 Hz, 2H), 7.71 (t, *J* = 7.5 Hz, 1H), 7.57 (t, *J* = 7.5 Hz, 2H), 7.45 (d, *J* = 9.1 Hz, 2H). ^{13}C{^{1}H} NMR (75 MHz, CDCl$_3$) δ: 164.1, 155.6, 145.3, 134.2, 130.2, 128.7, 128.4, 125.2, 122.5.

2-Hydroxy-5-methoxybenzophenone (1a). Pale yellow needles (188 mg; 94%). Mp: 83−84 °C (lit.[28] mp 84 °C). ^{1}H NMR (300 MHz, CDCl$_3$) δ: 11.58 (s, 3H); 7.69 (dd, *J* = 8.5, 1.6 Hz, 2H), 7.60 (t, *J* = 7.5 Hz, 1H), 7.51 (t, *J* = 7.8 Hz, 2H), 7.14 (d, *J* = 9.0, 2.9 Hz, 1H), 7.06 (d, *J* = 3.1 Hz, 1H), 7.02 (d, *J* = 9.0 Hz, 1H), 3.70 (s, 3H). ^{13}C{^{1}H} NMR (75 MHz, CDCl$_3$) δ: 201.1, 157.7, 151.6, 138.0, 132.1, 130.3, 129.2, 128.5, 124.3, 119.4, 116.5, 56.1.

2-Hydroxy-5-phenoxybenzophenone (2a). Yellow needles (193 mg; 76%). Mp: 47−48 °C. ^{1}H NMR (300 MHz, CDCl$_3$) δ: 11.85 (s, 1H), 7.70 (d, *J* = 8.1 Hz, 2H), 7.59 (t, *J* = 7.4 Hz, 1H), 7.50 (t, *J* = 7.6 Hz, 2H), 7.34−7.26 (m, 4 H), 7.12 (d, *J* = 8.7 Hz, 1H), 7.07 (t, *J* = 7.4 Hz, 1H), 6.94 (d, *J* = 8.7 Hz, 2H). ^{13}C{^{1}H} NMR (75 MHz, CDCl$_3$) δ: 200.9, 159.6, 158.6, 147.7, 137.5, 132.2, 129.8, 129.2, 128.9, 128.5, 123.8, 122.8, 119.7, 119.2, 117.3. Anal. Calcd for C$_{19}$H$_{14}$O$_3$: C, 78.61; H, 4.86. Found: C, 78.57; H, 4.90.

2-Hydroxy-5-methylbenzophenone (3a). Pale yellow needles (130 mg; 70%). Mp: 83−84 °C (lit.[29] mp 84 °C). ^{1}H NMR (300 MHz, CDCl$_3$) δ: 11.84 (s, 1H), 7.67 (dd, *J* = 8.4, 1.2 Hz, 2H), 7.60 (t, *J* = 7.4, 1H), 7.52 (t, *J* = 7.8 Hz, 2H), 7.36 (d, *J* = 2.8 Hz, 1 H), 7.32 (dd, *J* = 8.5,

2.3 Hz, 1H), 6.98 (d, *J* = 8.54 Hz, 1H), 2.28 (s, 3H).). ^{13}C{^{1}H} NMR (75 MHz, CDCl$_3$) δ: 201.7, 161.3, 138.2, 137.5, 133.3, 131.9, 129.2, 128.5, 127.9, 118.9, 118.3, 20.6.

2-Hydroxy-5-t-butylbenzophenone (4a). White solid (189 mg; 85%). M: 67−68 °C (lit.[25] mp 67−68 °C). ^{1}H NMR (300 MHz, CDCl$_3$) δ: 11.87 (s, 1 H), 7.72 (dd, *J* = 1.6, 8.1 Hz, 2H), 7.63 (t, *J* = 1.3, 7.4, 2H), 7.60 (t, *J* = 2.5, 8.5 Hz, 1H), 7.55 (t, *J* = 1.6, 7.2 Hz, 2 H), 7.05 (d, *J* = 8.3 Hz, 1H), 1.28 (s, 9H). ^{13}C{^{1}H} NMR (75 MHz, CDCl$_3$) δ: 201.6, 161.0, 141.3, 138.1, 133.9, 131.9, 129.8, 129.3, 128.3, 118.4, 117.9, 34.1, 31.3.

2-Hydroxybenzophenone (5a). Yellow needles (156 mg; 90%). Mp: 37−38 °C (lit.[6a] mp 37−38 °C). ^{1}H NMR (300 MHz, CDCl$_3$) δ: 12.05 (s, 1H), 7.68 (dd, *J* = 1.4, 8.4 Hz, 2H), 7.61−7.57 (m, 2H), 7.53−7.48 (m, 3H), 7.08 (dd, *J* = 1.1, 8.5 Hz, 1 H), 6.88 (dd, *J* = 1.1, 7.2 Hz, 1H). ^{13}C{^{1}H} NMR (75 MHz, CDCl$_3$) δ: 201.7, 163.3, 138.0, 136.4, 133.7, 132.0, 129.3, 129.2, 128.5, 119.2, 118.8, 118.5, 118.3.

4-Hydroxybenzophenone. Yellow plates (14 mg; 8%). Mp: 133−134 °C (lit.[6a,30] mp 133−134 °C). ^{1}H NMR (300 MHz, CDCl$_3$) δ: 7.77 (d, *J* = 8.8 Hz, 2H), 7.75 (d, *J* = 8.4 Hz, 2H), 7.57 (t, *J* = 7.4, 1.3 Hz, 1H), 7.47 (t, *J* = 7.5 Hz, 2 H), 6.95 (d, *J* = 8.7 Hz, 2H). ^{13}C{1H} NMR (75 MHz, CDCl$_3$) δ: 197.2, 161.1, 138.1, 133.3, 132.4, 130.0, 129.5, 128.4, 115.6.

2-Hydroxy-5-phenylbenzophenone (6a). White needles (209 mg; 87%). Mp: 91−92 °C (lit.[31] mp 91−92 °C). ^{1}H NMR (300 MHz, CDCl$_3$) δ: 12.06 (s, 1 H), 7.80 (dd, *J* = 2.4, 8.6 Hz, 1H), 7.77 (dd, *J* = 1.5, 8.5, 2H), 7.70−7.62 (m, 2H), 7.56 (t, *J* = 7.7, 1.7 Hz, 2H), 7.49 (dd, *J* = 8.5, 1.4 Hz, 2 H), 7.44 (t, *J* = 7.5, 1.5 Hz, 2H), 7.35 (t, *J* = 7.2 Hz, 1H), 7.21 (d, *J* = 8.6 Hz, 1H). ^{13}C{^{1}H} NMR (75 MHz, CDCl$_3$) δ: 201.7, 162.6, 139.8, 137.9, 135.1, 133.7, 132.1, 132.0, 131.8, 129.3, 128.9, 128.8, 128.5, 119.3, 118.9.

2-Hydroxy-5-cyanobenzophenone (7a). Pale yellow needles (156 mg; 80%). Mp: 120−121 °C (lit.[32] mp 120−121 °C). ^{1}H NMR (300 MHz, CDCl$_3$) δ: 12.48 (s, 1H), 7.96 (d, *J* = 2.1, 1H), 7.74 (dd, *J* = 8.7, 2.1 Hz, 1H), 7.70−7.65 (m, 3H), 7.60−7.55 (m, 2H), 7.16 (d, *J* = 8.7 Hz, 1H). ^{13}C{^{1}H} NMR (75 MHz, CDCl$_3$) δ: 200.6, 166.4, 138.7, 138.4, 136.6, 133.1, 129.3, 129.0, 120.2, 119.4, 118.3, 102.6.

2-Hydroxy-5-nitrobenzophenone (8a). Intense yellow plates (94 mg; 44%). Mp.: 123−124 °C (lit.[33] mp 123−124 °C). ^{1}H NMR (300 MHz, CDCl$_3$) δ: 12.67 (s, 1H), 8.60 (d, *J* = 2.7 Hz, 1H), 8.40 (dd, *J* = 9.2, 2.7 Hz, 1H), 7.72 (d, *J* = 8.4, 1.3 Hz, 2H), 7.69 (t, *J* = 7.5, 1.3 Hz, 1H), 7.59 (t, *J* = 7.8, 1.8 Hz, 2H), 7.19 (d, *J* = 9.2 Hz, 1H). ^{13}C{^{1}H} NMR (75 MHz, CDCl$_3$) δ: 200.7, 168.1, 139.6, 136.5, 133.3, 131.1, 129.8, 129.4, 129.2, 119.7, 118.1.

ASSOCIATED CONTENT

Ⓢ Supporting Information

AUTHOR INFORMATION

Corresponding Author

*E-mail: smbonesi@qo.fcen.uba.ar. Tel:+541145763346.

ORCID 🄳

Stefano Crespi: 0000-0002-0279-4903

Sergio M. Bonesi: 0000-0003-0722-339X

Notes

The authors declare no competing financial interest.

■ REFERENCES

(1) (a) Miranda, M. A.; Galindo, F. In *Photochemistry of Organic Molecules in isotropic and Anisotropic Media;*. Ramamurthy, V., Schanze, K. S., Eds.; Marcel Dekker: New York, 2003; Chapter 2. (b) Natarajan, A.; Kaanumale, L. S.; Ramamurthy, V. In *CRC Handbook of Organic Photochemistry and Photobiology*; Horspool, W., Lenci, F., Eds.; CRC Press: Boca Raton, FL, 2004; Vol. 3, p 107. (c) Fendler, J. H.; Fendler, E. J. In *Catalysis in Micellar and Macromolecular System*; Academic Press: London, 1975. (d) *Mixed Surfactant System*; Holland, P. M., Rubingh, D. N., Eds.; American Chemical Society: Washington, DC, 1994. (e) Turro, N. J. From Boiling Stones to Smart Crystals: Supramolecular and Magnetic Isotope Control of Radical−Radical Reactions in Zeolites. *Acc. Chem. Res.* **2000**, *33*, 637−646.

(2) (a) Turro, N. J.; Mattay, J. Photochemistry of some deoxybenzoines in micellar solution. Cage effects, isotop effects, and magnetic field effects. *J. Am. Chem. Soc.* **1981**, *103*, 4200−4204. (b) Turro, N. J.; Sidney Cox, G.; Paczkowski, M. A. *Photochemistry in Micelles in Topics in Current Chemistry, Photochemistry and Organic Synthesis*; Boschke, F. L., Ed.; Springer-Verlag: New York, 1985; Vol. *129*, p 57.

(3) (a) Turro, N. J.; Kraeutler, B. Magnetic field and magnetic isotope effects in organic photochemical reactions. A novel probe of reaction mechanisms and a method for enrichment of magnetic isotopes. *Acc. Chem. Res.* **1980**, *13*, 369−377. (b) Turro, N. J.; Buchachenko, A. L.; Tarasov, V. F. How spin stereochemistry severely complicates the formation of a carbon-carbon bond between two reactive radicals in a supercage. *Acc. Chem. Res.* **1995**, *28*, 69−80. (c) Lalyanasundaran, K. In *Photochemistry in Microheterogeneous Systems*; Academic Press: Orlando, FL, 1987.

(4) Anderson, J. C.; Reese, C. B. Photo-induced Fries rearrangement. *Proc. Chem. Soc. London* **1960**, 217.

(5) (a) Bellus, D. Photo-Fries rearrangement and related photochemical [1,j]-shifts (j = 3, 5, 7) of carbonyl and sulfonylgroups. *Adv. Photochem.* **2007**, *8*, 109−159. (b) Miranda, M. A. In *CRC Handbook of Organic Photochemistry and Photobiology*; Horspool, W., Song, P. S., Eds.; CRC Press: Boca Raton, FL, 1995; p 570. (c) Belluc, B.; Hdrlovic, P. Photochemical rearrangement of aryl, vinyl and substituted vinyl esters and amides of carboxylic acids. *Chem. Rev.* **1967**, *67*, 599−609. (d) Photo-Fries Rearrangement. In *Comprehensive Organic Name Reactions and Reagents*; Wiley, 2010; Vol. *497*, pp 2200−2205. (e) Kobsa, H. Rearrangement of aromatic esters by ultraviolet radiation. *J. Org. Chem.* **1962**, *27*, 2293−2298. (f) Sandner, M. R.; Trecker, D. J. Mechanism of the photo-Fries reaction. *J. Am. Chem. Soc.* **1967**, *89*, 5725−5726. (g) Consuelo Jimenez, M.; Miranda, M. A.; Scaiano, J. C.; Tormos, R. Two-photon processes in the photo-Claisen and photo-Fries rearrangements. Direct observation of diene ketenes generated by photolysis by transient cyclohexa-2,4-dienones. *Chem. Commun.* **1997**, 1487−1488. (h) Lochbrunner, S.; Zissler, M.; Piel, J.; Riedle, E. Real time observation of the photo-Fries rearrangement. *J. Chem. Phys.* **2004**, *120*, 11634−11639. (i) Norell, J. R. Organic reactions in liquid hydrogen fluoride. IV Fries rearrangement of aryl benzoates. *J. Org. Chem.* **1973**, *38*, 1924−1928. (j) Park, K. K.; Lee, J. J.; Ryu, J. Photo-Fries rearrangement of N-aryl sulfonamides to aminoaryl sulfone derivatives. *Tetrahedron* **2003**, *59*, 7651−7659.

(6) (a) Meyer, J. W.; Hammond, G. S. Mechanism of photochemical reactions in solution. LXX. Photolysis of aryl esters. *J. Am. Chem. Soc.* **1972**, *94*, 2219−2228. (b) Kalmus, C. E.; Hercules, D. S. Mechanistic studies of the photo-Fries rearrangement of phenyl acetate. *J. Am. Chem. Soc.* **1974**, *96*, 449−460. (c) Gritsan, N. P.; Tsentalovich, Y. P.; Yurkovskay, A. V.; Sagdeev, R. Z. Laser flash photolysis and CIDNP studies of 1-naphthyl acetate phto-Fries rearrangement. *J. Phys. Chem.* **1996**, *100*, 4448−4458. (d) Bonesi, S. M.; Crevatin, L. K.; Erra Balsells,

R. Photochemistry of 2-acyloxycarbazoles. A potential tool in the synthesis of carbazole alkaloids. *Photochem. Photobiol. Sci.* **2004**, *3*, 381−388. (e) Crevatin, L. C.; Bonesi, S. M.; Erra Balsells, R. Photo-Fries rearrangement of carbazol-2-yl sulfonates: efficient tool for the introduction of sulfonyl groups into polycyclic aromatic compounds. *Helv. Chim. Acta* **2006**, *89*, 1147−1157.

(7) (a) Sandner, M. R.; Hedaya, E.; Trecker, D. J. Mechanistic studies of the photo-Fries reaction. *J. Am. Chem. Soc.* **1968**, *90*, 7249−7254. (b) Coppinger, G. M.; Bell, E. R. Photo-Fries rearrangement of aromatic esters. Role of steric and electronic factors. *J. Phys. Chem.* **1966**, *70*, 3479−3489. (c) Sharma, P. K.; Khanna, N. R. Photo-Fries rearrangement: rearrangement of benzoyloxy compounds. *Monatsh. Chem.* **1985**, *116*, 353−356. (d) Finnegan, R. A.; Mattice, J. J. Photochemical studies. II. The photo rearrangement of aryl esters. *Tetrahedron* **1965**, *21*, 1015−1016. (e) Adam, W.; Sanabia, J. A.; Fischer, H. CIDNP evidence for radical pair mechanism in photo-Fries rearrangement. *J. Org. Chem.* **1973**, *38*, 2571−2572. (f) Adam, W. The multiplicity of the photo-Fries rearrangement. *J. Chem. Soc., Chem. Commun.* **1974**, 289−290. (g) Stumpe, J.; Selbmann, Ch.; Kreysig, D. Photoreactions in liquid crystal 2. Photo-Fries rearrangement of aromatic esters in liquid crystalline matrices. *J. Photochem. Photobiol., A* **1991**, *58*, 15−30.

(8) (a) Singh, A. K.; Raghuraman, T. S. Photorearrangement of phenyl cinnamates under micellar environment. *Tetrahedron Lett.* **1985**, *26*, 4125−4128. (b) Singh, A. K.; Raghuraman, T. S. Photorearrangement of aryl esters in micellar medium. *Synth. Commun.* **1986**, *16*, 485−490. (c) Xie, R. Q.; Liu, Y. C.; Lei, X. G. The photo-Fries rearrangement of α-naphthyl acetate in cyclodextrin and micelle. *Res. Chem. Intermed.* **1992**, *18*, 61−69. (d) Nassetta, M.; De Rossi, R. H.; Cosa, J. J. Influence of cyclodextrine on the photo-Fries rearrangement of acetanilide. *Can. J. Chem.* **1988**, *66*, 2794−2798. (e) Pitchumani, K.; Warrier, M.; Ramamurthy, V. Remarkable product selectivity during Photo-Fries and photo-claisen rearrangements within zeolites. *J. Am. Chem. Soc.* **1996**, *118*, 9428−9429.

(9) Iguchi, D.; Erra-Balsells, R.; Bonesi, S. M. Photo-Fries rearrangement of aryl acetamides: regioselectivity induced by the aqueous micellar green environment. *Photochem. Photobiol. Sci.* **2016**, *15*, 105−116.

(10) (a) Morohoshi, K.; Yamamoto, H.; Kamata, R.; Shiraishi, F.; Koda, T.; Morita, M. estrogenic activity of 37 componets of commercial sunscreen lotions evaluated by in vitro assays. *Toxicol. In Vitro* **2005**, *19*, 457−469. (b) Venu, T. D.; Shashikauth, S.; Khanun, S. A.; Naveen, S.; Firdouse, A.; Sridhar, M. A.; Shashidhara Prasad, J. Synthesis and crystallographic analysis of benzophenone derivatives. The potential anti-inflammatory agents. *Bioorg. Med. Chem.* **2007**, *15*, 3505−3514. (c) Coronado, M.; De Haro, H.; Deng, X.; Rempel, M. A.; Lavado, R.; Schlenck, D. Estrogenic activity and reproductive effects of the UV-filter oxybenzone (2-hydroxy-4-methoxyphenyl-methanone) in fish. *Aquat. Toxicol.* **2008**, *90*, 182−187. (d) Maciel-Rezende, C. M.; de Almeida, L.; Costa, E. D.; Robeiro Pires, F.; Ferreira Alves, K.; Viegas Junior, C.; Ferreira Dias, D.; Dominguetto, A. C.; Marques, M. J.; Dos Santos, M. H. Synthesis and biological evaluation against *Leishmania amazonensis* of a series of alkyl-substituted benzophenones. *Bioorg. Med. Chem.* **2013**, *21*, 3114−3119.

(11) (a) Tachikawa, Y.; Cui, L.; Matsusaki, Y.; Tada, N.; Miura, T.; Itoh, A. Aerobic photooxidative cleavage of 1,3-diketones to carboxylic acids using 2-chloroanthraquinone. *Tetrahedron Lett.* **2013**, *54*, 6218−6221. (b) McNesby, J. R.; Heller, C. A. Oxidation of liquid aldehydes by molecular oxygen. *Chem. Rev.* **1954**, *54*, 325−346.

(12) Goldstein, S.; Rabani, J. The ferrioxalate and iodide-iodate actinometers in the UV region. *J. Photochem. Photobiol., A* **2008**, *193*, 50−55.

(13) Dichiarante, V.; Dondi, D.; Protti, S.; Fagnoni, M.; Albini, A. A meta effect in organic photochemistry? The case of S_N1 reactions in methoxyphenyl derivatives. *J. Am. Chem. Soc.* **2007**, *129*, 5605−5611; Correction: *J. Am. Chem. Soc.* **2007**, *129*, 5605−5611.

(14) (a) Turro, N. J. In *Modern Molecular Photochemistry*; The Benjamin Cummings Publishing Company: Menlo Park, CA, 1978. (b) Turro, N. J.; Ramamurthy, V.; Scaiano, J. C. In *Modern Molecular*

Photochemistry of Organic Molecules; University Science Books: Sausalito, CA, 2010.

(15) (a) Bonesi, S. M.; Mesaros, M.; Cabrerizo, F. M.; Ponce, M. A.; Bilmes, G.; Erra Balsells, R. The photophysics of nitrocarbazoles used as UV-MALDI matrices: comparative spectroscopic and optoacoustic studies of mononitro- and dinitrocarbazoles. *Chem. Phys. Lett.* **2007**, *446*, 49−55. (b) Cors, A.; Bonesi, S. M.; Erra Balsells, R. Photoreduction of nitro arenes by formic acid in acetonitrile at room temperature. *Tetrahedron Lett.* **2008**, *49*, 1555−1558.

(16) (a) Sepulveda, L.; Lissi, E.; Quina, F. H. Interactions of Neutral Molecules with Ionic Micelles. *Adv. Colloid Interface Sci.* **1986**, *25*, 1−57. (b) Quina, F. H.; Alonso, E. O. Incorporation of Nonionic Solutes into Aqueous Micelles: A Linear Solvation Free Energy Relationship Analysis. *J. Phys. Chem.* **1995**, *99*, 11708−11714. (c) Abraham, H.; Chadha, H. S.; Dixon, J. P.; Rafols, C.; Treiner, C. Hydrogen bonding Part 40. Factors that influence the distribution of solutes between water and sodium dodecylsulfate micelles. *J. Chem. Soc., Perkin Trans. 2* **1995**, *2*, 887−894. (d) Abraham, H.; Chadha, H. S.; Dixon, J. P.; Rafols, C.; Treiner, C. Hydrogen bonding. Part 41.1 Factors that influence the distribution of solutes between water and hexadecylpyridinium chloride micelles. *J. Chem. Soc., Perkin Trans. 2* **1997**, 19−24.

(17) Brinchi, L.; di Profio, P.; Micheli, F.; Germani, R.; Savelli, G.; Bunton, C. A. Structure of Micellar head-Groups and the Hydrolysis of Phenyl Chloroformate. The Role of Perchlorate Ion. *Eur. J. Org. Chem.* **2001**, *2001*, 1115.

(18) Campos Rey, P.; Cabaleiro Lago, C.; Hervés, P. Solvolysis of Substituted benzoyl Chlorides in Nonionic and Mixed Micllar Solutions. *J. Phys. Chem. B* **2010**, *114*, 14004−14011.

(19) (a) Sabatino, P.; Szczygiel, A.; Sinnaeve, D.; Hakimhashemi, M.; Saveyn, H.; Martins, J. C.; van der Meeren, P. NMR study of the influence of pH on phenol sorption in cationic CTAB micellar solutions. *Colloids Surf., A* **2010**, *370*, 42−48. (b) Voets, I. K.; de Keizer, A.; de Waard, P.; Frederik, P. M.; Bomans, P. H. H.; Schmalz, H.; Walther, A.; King, S. M.; Leermakers, F. A. M.; Cohen Stuart, M. A. Doubled-faced micelles from water-soluble polymers. *Angew. Chem., Int. Ed.* **2006**, *45*, 6673−6676. (c) Yuan, H. Z.; Zhao, S.; Cheng, G. Z.; Zhang, L.; Miao, X. J.; Mao, S. Z.; Yu, J. Y.; Shen, L. F.; Du, Y. R. Mixed micelles of Triton X-100 and Cetyl triammonium bromide in aqueous solution studied by 1h NMR. *J. Phys. Chem. B* **2001**, *105*, 4611−4615.

(20) (a) Das, P. K.; Encinas, M. V.; Steenken, S.; Scaiano, J. C. Reaction of t-butoxy radicals with phenols. Comparison with the reactions of carbonyl triplets. *J. Am. Chem. Soc.* **1981**, *103*, 4162−4166. (b) Land, E. J.; Porter, G.; Strachan, E. Primary photochemical processes in aromatic molecules. Part 6. The absorption spectra and acidity constants of phenoxyl radicals. *Trans. Faraday Soc.* **1961**, *57*, 1885−1893. (c) Land, E. J.; Porter, G. Primary photochemical processes in aromatic molecules. Part 7. Spectra and kinetics of some phenoxyl derivatives. *Trans. Faraday Soc.* **1963**, *59*, 2016−2026. (d) Land, E. J.; Ebert, M. Pulse radiolysis studies of aqueous phenol. Water elimination from dihydroxycyclohexadienyl radicals to form phenoxyl. *Trans. Faraday Soc.* **1967**, *63*, 1181−1190. (e) Gadosy, T. A.; Shukla, D.; Johnston, L. J. Generation, characterization, and deprotonation of phenol radical cations. *J. Phys. Chem. A* **1999**, *103*, 8834−8839. (f) Alfassi, Z. B.; Schuler, R. H. Reaction of azide radicals with aromatic compounds. Azide as a selective oxidant. *J. Phys. Chem.* **1985**, *89*, 3359−3363. (g) Ganapathi, M. R.; Hermann, R.; Naumov, S.; Brede, O. free electron transfer from several phenols to radical cations of non-polar solvents. *Phys. Chem. Chem. Phys.* **2000**, *2*, 4947−4955.

(21) Bonesi, S. M.; Crespi, S.; Merli, D.; Manet, I.; Albini, A. Direct irradiation of aryl sulfides: hemolytic fragmentation and sensitized S-oxidation. *J. Org. Chem.* **2017**, *82*, 9054−9065.

(22) Chen, C.-T.; Munot, Y. S. Direct atom-efficient esterification between carboxylic acids and alcohols catalyzed by atmospheric, water-tolerant TiO(acac)$_2$. *J. Org. Chem.* **2005**, *70*, 8625−8627.

(23) Seni, A. A.; Kollar, L.; Mika, L. T.; Pongracz, P. Rhodium-catalysed aryloxycarbonylation of iodo-aromatics by 4-substituted phenols with carbon monoxide or paraformaldehyde. *Molecular Catalysis* **2018**, *457*, 67−73.

(24) Singh, A. K.; Sonar, S. M. Photorearrangement of aryl esters in micellar medium. *Synth. Commun.* **1985**, *15*, 1113−1122.

(25) Kobsa, H. Rearrangement of Aromatic esters by ultraviolet radiation. *J. Org. Chem.* **1962**, *27*, 2293−2298.

(26) (a) Arisawa, M.; Igarashi, Y.; Kobayashi, H.; Yamada, T.; Bando, K.; Ichikawa, T.; Yamaguchi, M. Equilibrium shift in the rhodium-catalyzed acyl transfer reactions. *Tetrahedron* **2011**, *67*, 7846−7859. (b) Neuvonen, H.; Neuvonen, K.; Pasanen, P. Evidence of Substituent-Induced Electronic Interplay. Effect of the Remote Aromatic Ring Substituent of Phenyl Benzoates on the Sensitivity of the Carbonyl Unit to Electronic Effects of Phenyl or Benzoyl Ring Substituents. *J. Org. Chem.* **2004**, *69*, 3794−3800.

(27) Kim, S.; Lee, J. I.; Kim, Y. C. A simple and mild esterification method for carboxylic acids using mixed carboxylic-carbonic anhydrides. *J. Org. Chem.* **1985**, *50*, 560−565.

(28) Martin, R. Studies on the Friedel-Craft reaction. Preparation of isomeric 2-acyl- and 3-acyl-4-methoxy phenols. *Monatsh. Chem.* **1981**, *112*, 1155−1163.

(29) Sandner, M. R.; Hedaya, E.; Trecker, D. J. Mechanistic studies of the photo-Fries rearrangement. *J. Am. Chem. Soc.* **1968**, *90*, 7249.

(30) Cheung, C. W.; Buchwald, S. L. Palladium-catalyzed hydroxylation of aryl and heteroarylhalides enabled by the use of a Palladacycle precatalyst. *J. Org. Chem.* **2014**, *79*, 5351−5358.

(31) (a) Gu, Y.; Wu, F.; Yang, J. Oxidative [3 + 3] annulation of atropaldehyde acetals with 1,3-bisnuclophiles: an efficient method of constructing six-membered aromatic rings, including salicylates and carbazoles. *Adv. Synth. Catal.* **2018**, *360*, 2727−2741. (b) Xie, Y. Acylation of Csp2-H bond with acyl sources derived from alkynes Rh-Cu bimetallic catalyzed C-C bond cleavage. *Chem. Commun.* **2016**, *52*, 12372−12375.

(32) Yaegashi, T.; Nunomura, S.; Okutome, T.; Nakayama, T.; Kurumi, M.; Sakurai, Y.; Aoyama, T.; Fujii, S. Synthesis and structure-activity of protease inhibitors. III. Amidinophenols and their benzoyl esters. *Chem. Pharm. Bull.* **1984**, *32*, 4466−4477.

(33) Martin, R. *Substituted Hydroxybenzophenone (Class of Methanones) in Aromatic Hydroxyketones: Preparation and Physical Properties*; Springer: Dordrecht, 2011.